A molecular scheme for the reaction between acetylcholine and nicotinic channels

Ch. Franke,* H. Parnas,‡ G. Hovav,‡ and J. Dudel*

*Physiologisches Institut der Technischen Universität, 8000 München 40, Germany; and ‡Otto-Loewi-Center, Department of Neurobiology, Hebrew University, Jerusalem, Israel

ABSTRACT In outside-out patches of mouse-muscle membrane, embryonic-like channels were activated by pulses of acetylcholine (ACh). On increasing the ACh concentration, the rate of desensitization, $1/\tau_d$, increased linearly with the peak open probability, indicating desensitization from the open state. Desensitization had only one time constant τ_d at each ACh concentration. Recovery from desensitization was only ~10 times slower than desensitization, whereas the probability of steady-state channel opening, declined to <0.01 with >10^{-6} M ACh. The peak probability of opening in >10^{-4} M ACh pulse was close to 1. A linear reaction scheme was not compatible with these results. The scheme had to be expanded resulting in a circular scheme with two additional ACh binding steps to desensitized channel states. The approximate rate constants of all reaction steps in the circular scheme could be determined using computer simulations. The model predicted that clusters of channel opening had the average duration τ_d at the respective ACh concentration. In cell-attached patches on intact muscle fibers, similar average cluster durations were observed at the respective ACh concentration. This indicates that τ_d in the intact muscle fibers has similar values as in outside-out patches.

INTRODUCTION

Desensitization of nicotinic endplate receptors in the sustained presence of the transmitter acetylcholine (ACh) has been described by Fatt (1950) and Thesleff (1955). In a seminal article, Katz and Thesleff (1957) have measured the time course and the degree of desensitization by applying a steady dose of ACh from one barrel of a microelectrode, and a superimposed series of short pulses of ACh from a second barrel. Desensitization was defined as the decline of the responses to the ACh pulses during the application of the continuous ACh dose. After washout of ACh, the growing responses to the pulses indicated recovery from desensitization. Katz and Thesleff (1957) discussed several reaction schemes for desensitization. A "circular" reaction scheme suggested by them has been developed further in several modifications. The scheme involved binding of ACh both to the nondesensitized and to the desensitized state of the receptor.

Patch-clamp recordings from channels from the endplate have shown that there are two consecutive binding reactions of ACh to the nondesensitized receptor, which are followed by rapidly oscillating conformational changes to an open channel state and back (see Colquhoun and Sakman, 1985). Circular desensitization schemes derived from the one of Katz and Thesleff (1957) have included these activation characteristics (see Cachelin and Colquhoun, 1989). The desensitization literature was reviewed recently by Scuka and Mozrzymas (1992). The studies discussed so far used steady-state effects of ACh or relatively slow techniques of application of ACh. They found "rapid" time constants of desensitization in the 1-s range.

Direct measurements of the activation, desensitization, and recovery time course of nicotinic ACh receptors became possible with rapid applications of ACh to outside-out patches of membrane. Far more rapid desensitization and recovery was found than observed so far in superfusions of endplates (Dilger and Brett 1990; Franke et al. 1991a, b, 1992b; Dilger and Liu 1992). The new data on the single channel level are used in the present article for an analysis of the possible routes of desensitization in nicotinic ACh receptors. We shall demonstrate that a circular scheme is unavoidable and try to determine all the rate constants of this scheme.

METHODS

The preparations were toe muscles of the mouse that were cultured for 14 d and developed ACh-receptors of the embryonic-like type during this period (Franke et al., 1992b). Alternatively, myotubes were produced from hindleg muscles of 8–10-d old mice in a procedure modified from Blan and Webster (1981). The muscles were minced with fine scissors and incubated for 1 h at 37°C in 10 ml of Ham's F-12 standard tissue culture medium (Serva Biochemicals, Paramus, NJ), which contained 15 mg collagenase type V, 20 mg protease, and 5 mg desoxyribonuclease (all Sigma Chemical Co., St. Louis, MO). Thereafter, the dissociated muscles were triturated and centrifuged at 500 rotations/min. The pellet was resuspended in F-12 medium with 20% fetal calf serum (Serva Biochemicals) and distributed into tissue culture dishes that had been collagenated with rat-tail collagen; the cells were cultured for up to 4 d until forming a confluent layer. Changing the medium to Dulbecco's modified Eagle's medium (Sigma Chemical) with 5% fetal calf serum and 5% horse serum induced fusion of myoblasts and formation of myotubes within 2–4 d. The myotubes showed central nuclei and contracted spontaneously. Finally, 1–5 mg/ml Cytosin arabinoside (Sigma Chemical) were added to stop further growth of fibroblasts.

Outside-out patches of membrane were prepared from both the muscle cell cultures and the myotubes (Hamill et al., 1981). The prepara-

tions were held at ~20°C. The patches were superfused with pulses of ACh by means of a liquid filament switch (Franke et al., 1987; Dudel et al. 1990a). Only channel openings of the embryonic-like type with a single channel conductance of 37 pS (Franke et al., 1992a) were observed. Patch-clamp recording, data storage, and evaluation were performed as described in Franke et al. (1991b). Very low average channel opening rates had to be determined in experiments using low ACh concentrations or strongly desensitized channels in long-time applications of ACh. Under these conditions, averaging of responses by synchronized adding of traces may amplify small artefacts, for instance, current offsets generated by the application system. Therefore, the recorded single traces that contained few superpositions of openings were fed into an "ideal trace" program. This program detected single or (low) multiples of openings and generated corresponding pulses with amplitudes of one, two, and three channels (Dudel et al., 1990b). After eliminating artefacts in this manner, proper averages were formed.

Simulation of the reaction scheme was done by two methods. One program (Parnas et al., 1989) solved the sets of differential equations valid for the different schemes for suitable intervals of time after application of ACh using the fourth order Runge-Kutta method. The time course of the probabilities of the different channel states after a pulse of ACh could be plotted for different sets of rate constants. A second program modeled the stochastic changes in the states of single channels. A random generator of numbers between 0 and 1 was used. For each small time interval, dt, the selected random number and the transition probabilities from a certain channel state decided whether one and which transition would take place. Such stochastic simulations generate a list of times at which the channel opens or closes. From this data, open-time histograms, burst-time histograms, and so on could be plotted and compared with the experimental results, using the same criteria as used for the evaluation of the patch-clamp data. The simulations also predict the peak open probability of opening ($p_{o, max}$), the steady-state probability of opening ($p_{o, ss}$), and the time constant of desensitization (τ_d). The simulations were written and performed on SUN and IBM 486 computers.
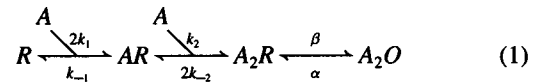
RESULTS

Experimental dose-response curves

Dose-response curves from three typical experiments for the peak current, $p_{o, max}$, and for the time constant of desensitization, τ_d, are given in Fig. 1, A and B. The data were derived from original recordings, in which ACh was applied repetitively in pulses of 0.5–1 s duration, which was repeated with different ACh concentrations in the same patch (see Figs. 4 and 8). The ordinate in Fig. 1 A is $p_{o, max}$, the peak probability for one channel to be open. In these plots, $p_{o, max}$ with 10^{-3} M ACh was taken to be 1. As will be shown below (see Fig. 8), the peak open probability with 10^{-3} M ACh is ~0.96. The dose-response curves for $p_{o, max}$ rise with a double-logarithmic slope > 1 up to ~10^{-5} M ACh and approach saturation above this concentration (see also Franke et al., 1992b).

The dose-response curves for the rate of desensitization, $1/\tau_d$, have the same shape as those for $p_{o, max}$ (Fig. 1 B). This is more obvious in Fig. 1 C, in which $1/\tau_d$ is plotted versus $p_{o, max}$. In each of the experiments, $1/\tau_d$ was proportional to $p_{o, max}$. The proportionality factors vary between 20 and 80, reflecting considerable variation of τ_d in different samples of channels.

Schemes of desensitization of the nicotinic ACh receptor

For the activation or opening of nicotinic, ACh liganded channels scheme 1 seems to be accepted (Colquhoun and Sakman 1985, 1988; Sine and Steinbach 1986, 1987; Jackson 1988; Franke et al., 1991b; Dilger and Liu 1992):

$$R \underset{k_{-1}}{\overset{2k_1}{\rightleftarrows}} AR \underset{2k_{-2}}{\overset{k_2}{\rightleftarrows}} A_2R \underset{\alpha}{\overset{\beta}{\rightleftarrows}} A_2O \qquad (1)$$

In this scheme, R denotes the closed receptor-channel, A the agonist (ACh), and O the open receptor-channel. The rate constants were determined for the embryonic-like channels of mice in Franke et al. (1991b), but we increased $k_1 = k_2$ from 10^8 M^{-1} s^{-1} to 1.5×10^8 M^{-1} s^{-1} for reasons given later The scheme is simplified in two respects. (a) Colquhoun and Sakman (1985) have shown that the channel opens also from AR to a state AO. The AO openings are short and relatively rare, occur mainly at low ACh concentrations, and their contribution to the dose-response curves is almost negligible (Franke et al., 1991b). (b) Colquhoun and Sakmann (1985) also have included an intermittent channel block in which binding of ACh proceeds from A_2O. This channel block is effective at ACh concentrations > 10^{-4} M and at membrane potentials more negative than -70 mV. The results in our studies were obtained with outside-out patches clamped to potentials more positive than -50 mV, and in this potential range the intermittent block is not observed. Since the potential range < -70 mV is of minor relevance for the functional range of the endplate receptors, the complication of the scheme with the intermittent blocking step seemed unnecessary.

In reaction scheme 1, any of the states R to A_2O could be converted into a desensitized state, D to A_2D, either by binding of ACh or by a conformational change. Since the desensitization did not proceed with time constants shorter than 10 ms, the dose-response curve for $p_{o, max}$ is not affected. This curve is simulated in Fig. 2 A and is valid for scheme 1 as well for the desensitization schemes in Fig. 2, C and D. With respect to the rate of desensitization, $1/\tau_d$, the critical experimental finding is the linear relation between $p_{o, max}$ and $1/\tau_d$ (Fig. 1 C). Fig. 2, B–D presents simulations of this relationship for three desensitization schemes. In B and C, desensitization is produced by the binding of ACh. However, when desensitization starts from the open state by a conformational change $A_2O \rightleftarrows A_2D$ (Fig. 2 D), $1/\tau_d$ is proportional to $p_{o, max}$ as found experimentally (Fig. 1 C). The states A_2O and A_2R are in equilibrium, and therefore also a desensitization reaction $A_2R \rightleftarrows A_2D$ produces a linear relationship as in Fig. 2 D (An identical curve is generated, if the rate $A_2R \rightleftarrows A_2D$ is taken to be higher than d_1 in Fig. 2 D by a factor of $p_{o, max}/p_{A2R}$.) To complete the

Po, max

A

(Figure A: y-axis Po, max from 0.0001 to 1; x-axis 10^{-7} to 10^{-3})

1/τ$_d$ (s^{-1})

B

(Figure B: y-axis 1/τ$_d$ (s^{-1}) from 0.1 to 100; x-axis ACh concentration (M) 10^{-7} to 10^{-3})

ACh concentration (M)

1/τ$_d$ (s^{-1})

C

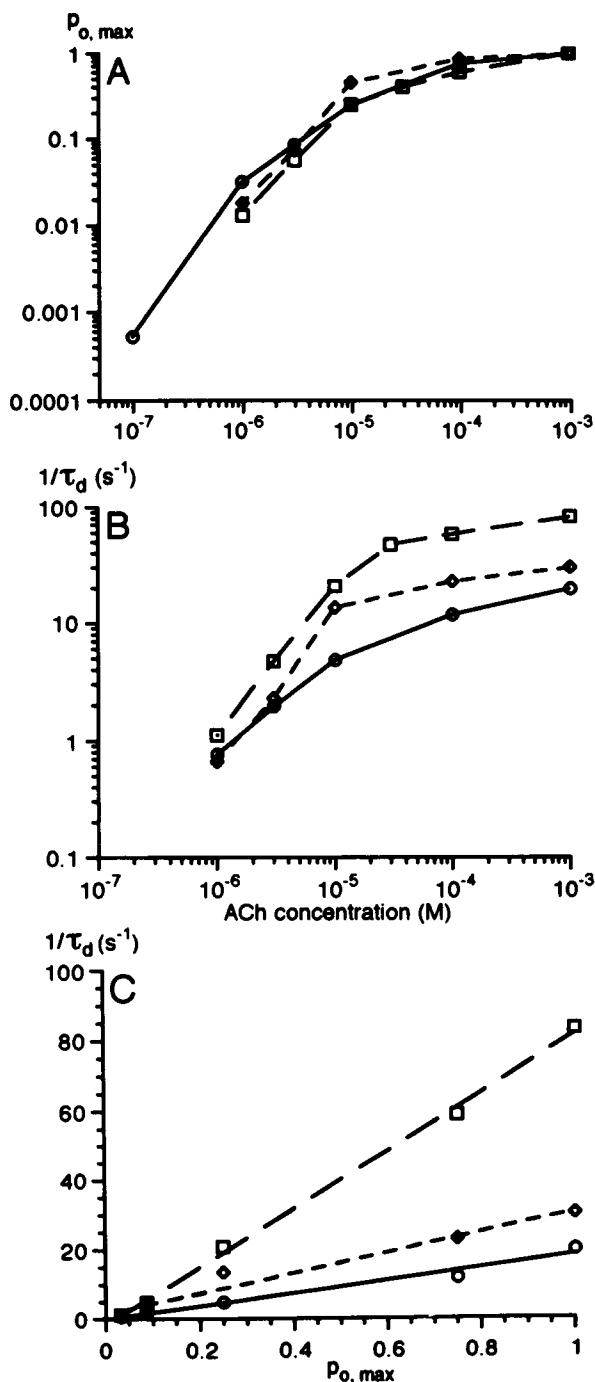(Figure C: y-axis 1/τ$_d$ (s^{-1}) 0 to 100; x-axis Po, max 0 to 1)

Po, max

FIGURE 1   (A and B) Dose-response curves for the maximal probability of channel opening $p_{o, max}$ and the rate of desensitization, $1/\tau_d$, for pulses of different ACh concentrations (abscissae) for three patches (□, ◇, and ○). $p_{o, max}$ elicited by 10^{-3} M ACh was assumed to be 1 (see text). (C) Plot of $1/\tau_d$ versus $p_{o, max}$ with the values from A and B.

discussion of possible desensitization schemes, desensitization by $AR \rightleftharpoons AD$ generates a nonlinear relation between $p_{o, max}$ and $1/\tau_d$ (not illustrated), and desensitization $R \rightleftharpoons D$ would decrease with increasing channel opening, since R would become less probable. Therefore, only desensitization by a conformational change

from A_2O (Fig. 2 D) or from A_2R conform to the experimental data in Fig. 1.

Monoexponential desensitization

The reaction scheme of Fig. 2 D contains only one time constant of desensitization. Many investigations have reported several time constants (see for instance Feltz and Trautmann, 1982; Cachelin and Colquhoun, 1989) and have given reaction models containing several desensitization time constants. Therefore, we have plotted measured desensitizations semilogarithmically, as illustrated in Fig. 3. Down to the limits given by the current noise, the time course of desensitization was found to be monoexponential. The plots in Fig. 3 extended over three to four time constants, to open probabilities < 0.05. Smaller slow components cannot be excluded by measurements like those in Fig. 3, and there are some indications for a very small, slow component of desensitization (see below).

Fig. 3 further stresses the variability of desensitization time constants from patch to patch (see also Franke et al., 1991a, 1992b). Two extreme values of τ_d, 10 and 61 ms, and a medium value, 22 ms, were selected. There is no difference in stability in patches with different desensitization time constants, and there is also no correlation between τ_d and the rate of rise of the initial response to ACh, which is two orders of magnitude faster than desensitization. The different τ_d values thus are not experimental artefacts but genuine characteristics of the respective channels.

Termination of channel opening and recovery from desensitization after an ACh pulse

During a pulse of 10^{-5} to 10^{-3} M, ACh channel opening declined rapidly after a peak response, approaching a steady-state level of desensitization that is $\sim 1/100$ or less of the peak (Fig. 4). When ACh was washed off at the end of the pulse, channel opening stopped almost immediately (compare also Franke et al., 1992a, b; Dilger and Liu, 1992). In the first recording of Fig. 4, a burst of openings of one channel continued for a few milliseconds after the end of the ACh pulse, but completion of bursts of channel opening was the only opening activity seen after washout of ACh. Late openings of channels after removing ACh were never observed, even if hundreds of channels were opened at the beginning of the ACh pulse.

After the termination of a pulse of ACh, the desensitized channels recover and reach the activatable resting state. The time course of this recovery was measured by recording the effects of double pulses of ACh applied with varying time intervals (Fig. 5 A). The first pulse produced a certain level of desensitization, and the response to the second pulse, which contained the same ACh concentration, indicated the level of desensitization
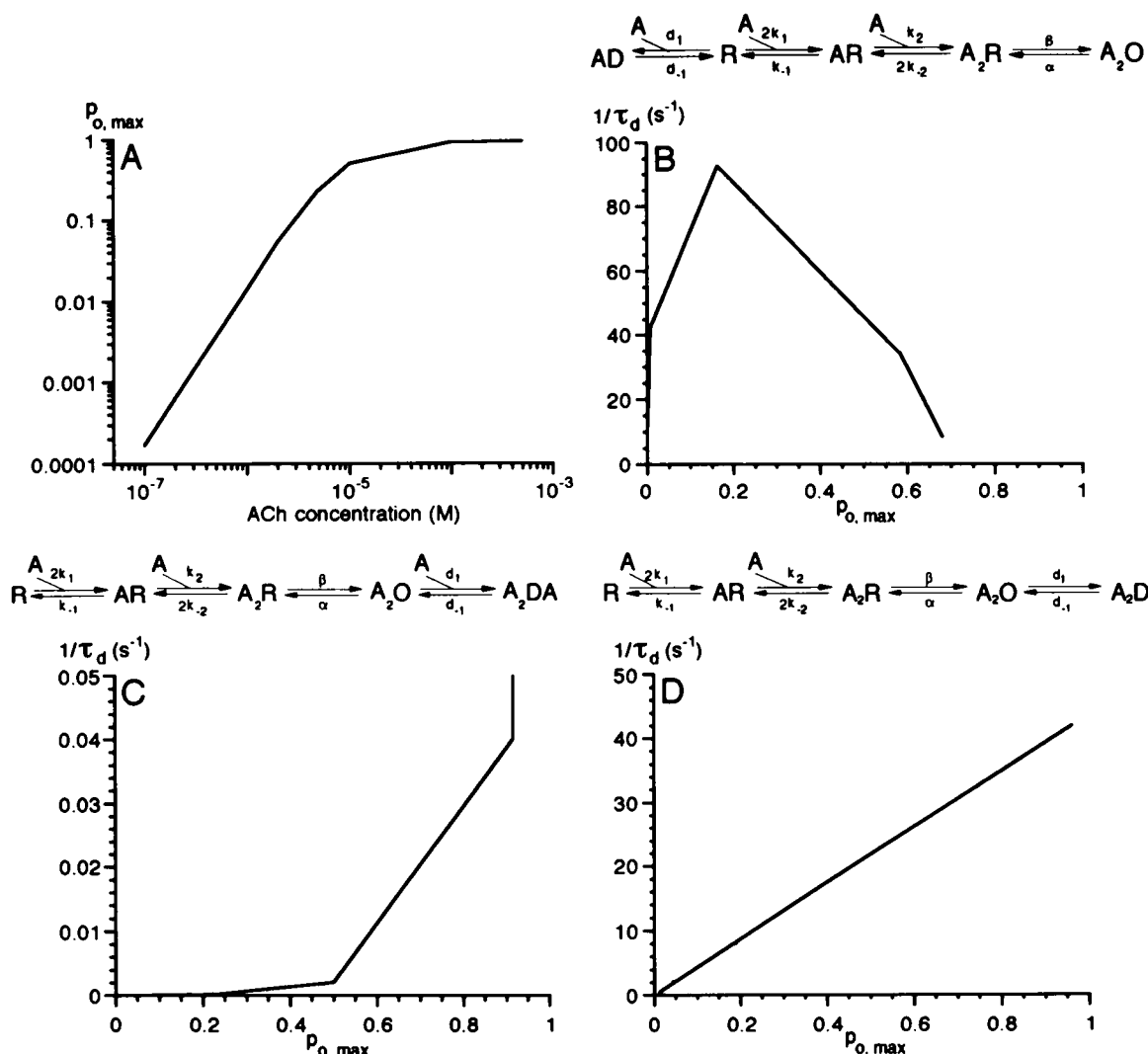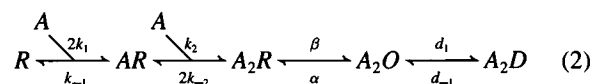
$$AD \underset{d_{-1}}{\overset{A \quad d_1}{\rightleftharpoons}} R \underset{k_{-1}}{\overset{A \quad 2k_1}{\rightleftharpoons}} AR \underset{2k_{-2}}{\overset{A \quad k_2}{\rightleftharpoons}} A_2R \underset{\alpha}{\overset{\beta}{\rightleftharpoons}} A_2O$$

$p_{o, max}$ / A

0.1

0.01

0.001

0.0001

10^{-7} 10^{-5} 10^{-3}

ACh concentration (M)

$1/\tau_d$ (s^{-1}) / B

100

80

60

40

20

0

0   0.2   0.4   0.6   0.8   1

$p_{o, max}$

$$R \underset{k_{-1}}{\overset{A \quad 2k_1}{\rightleftharpoons}} AR \underset{2k_{-2}}{\overset{A \quad k_2}{\rightleftharpoons}} A_2R \underset{\alpha}{\overset{\beta}{\rightleftharpoons}} A_2O \underset{d_{-1}}{\overset{A \quad d_1}{\rightleftharpoons}} A_2DA$$

$1/\tau_d$ (s^{-1}) / C

0.05

0.04

0.03

0.02

0.01

0

0   0.2   0.4   0.6   0.8   1

$p_{o, max}$

$$R \underset{k_{-1}}{\overset{A \quad 2k_1}{\rightleftharpoons}} AR \underset{2k_{-2}}{\overset{A \quad k_2}{\rightleftharpoons}} A_2R \underset{\alpha}{\overset{\beta}{\rightleftharpoons}} A_2O \underset{d_{-1}}{\overset{d_1}{\rightleftharpoons}} A_2D$$

$1/\tau_d$ (s^{-1}) / D

50

40

30

20

10

0

0   0.2   0.4   0.6   0.8   1

$p_{o, max}$

FIGURE 2   (A) Dose-response curve for the maximal probability of channel opening, $p_{o, max}$, calculated for the reactions schemes in B, C, and D (the result was identical). (C-D) Plot of $1/\tau_d$ versus $p_{o, max}$, calculated for the reaction schemes shown.

after the respective interval. The relative current amplitude, i.e., $p_{o, max}$ after pulse 2 divided by $p_{o, max}$ after pulse 1, is plotted in Fig. 5 B for three experiments. This relative current rose steeply between 50 and 500 ms after the prepulse and approached the control level above 1-s pulse interval. If one assumes an approximately exponential time course of recovery from desensitization, the time constant of recovery was 300–500 ms (see also Franke et al., 1992a).

Reaction scheme describing the termination of channel opening on removal of ACh and recovery from desensitization

We have established above that desensitization starts from the open state A_2O or from A_2R that is in rapid equilibrium with A_2O. Reaction scheme 2 represents the first of these possibilities (see Fig. 2 C):

$$R \underset{k_{-1}}{\overset{A \quad 2k_1}{\rightarrow}} AR \underset{2k_{-2}}{\overset{A \quad k_2}{\rightarrow}} A_2R \underset{\alpha}{\overset{\beta}{\rightarrow}} A_2O \underset{d_{-1}}{\overset{d_1}{\rightarrow}} A_2D \quad (2)$$

D denotes the desensitized state of the channel. The activation rate constants have the standard values: $k_1 = k_2 = 1.5 \times 10^8$ M^{-1} s^{-1}, $k_{-1} = k_{-2} = 8,000$ s^{-1}, $\alpha = 700$ s^{-1}, and $\beta = 30,000$ s^{-1} (Colquhoun and Sakmann, 1985; Franke et al., 1991b). The desensitization rate is $d_1 = 20$ s^{-1}, which will result in a time constant of desensitization of ~ 50 ms at high ACh concentration. A recovery rate $d_{-1} = 2$ s^{-1} is assumed that will generate half recovery from desensitization after ~ 300 ms (Fig. 5). However, two properties of the model are in conflict with the experimental results (Fig. 6 A). First, the steady-state level of channel opening, $p_{o, ss}$, was about 1/10 of the peak response, $p_{o, max}$, since $d_{-1}/d_1 = 1/10$. In the exper-

10^{-4} M ACh
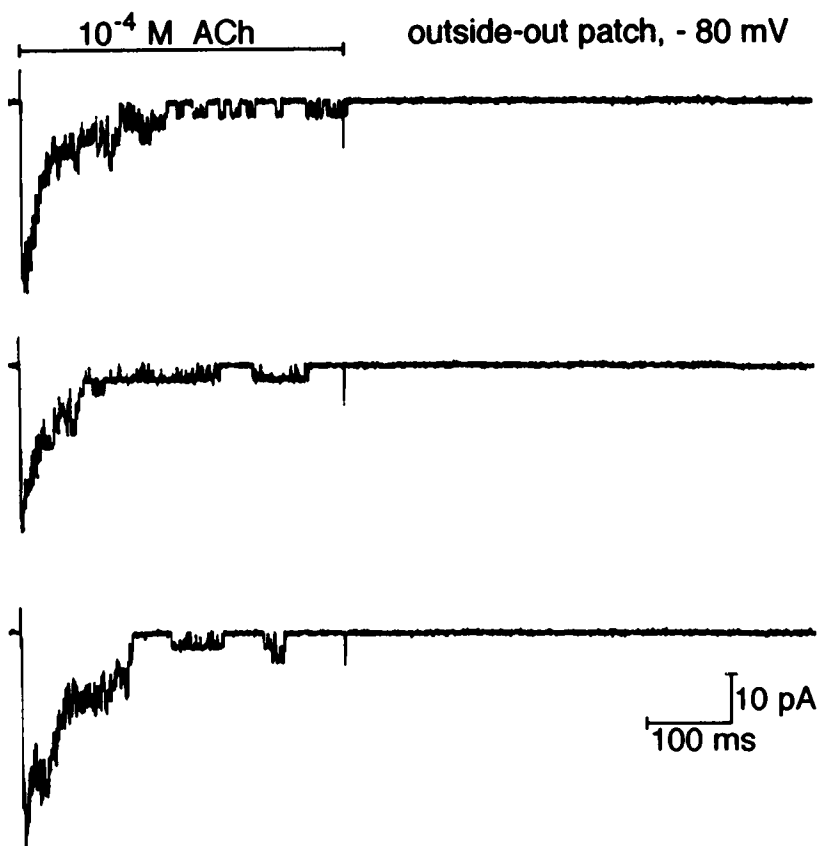
10^{-4} M ACh

10^{-4} M ACh

100 pA

100 ms

50 pA

100 ms

10 pA

20 ms

relative current amplitude

1
0.5
0.2
0.1
0.05

0   50   100   ms

61 ms

1
0.5
0.2
0.1

0   20   40 ms

22 ms

1
0.5
0.2
0.1
0.05

0   10   20   30 ms

10 ms

FIGURE 3 Average currents elicited by pulses of 10^{-4} M ACh during the marked periods of time in three different patches. To the right of each current trace, the decay of the maximal current (amplitude 1) is plotted semilogarithmically, and the time constant τ_d corresponding to the slope of the decay is indicated. The average currents contained 14–24 single records.

iments, $p_{o,ss}$ was $1/100$ or less of $p_{o,max}$ (Fig. 1). A 10 times lower d_{-1} value would have corrected the unrealistically high $p_{o,ss}$ but would have generated a 10 times slower time course of recovery from desensitization. Another serious conflict between the simulation of scheme 2 and the experimental results are channel openings long after washing out of ACh that are predicted by scheme 2. If the time period around the termination of the ACh pulse in Fig. 6 A is plotted with extended scales (Fig. 6 B), at the end of the ACh pulse, at 400 ms, openings decline first with a short time constant that corresponds to the burst duration of 2.7 ms in scheme 2 (see Colquhoun and Hawkes, 1981, Eq. 2.23).

In scheme 2, all the recovery from the desensitized state A_2D goes with the rate d_{-1} through the open state A_2O, and all channels will have to open on the average for at least one burst before returning to R. However, the experiments have shown that there are no openings of channels after washing off ACh (Fig. 4). A level of openings of 0.01 or even down to 0.00001 would have been easily detected; such low levels of p_o are observed in the steady-state activation of ACh in adult channels (Franke

et al., 1991a). It is concluded that the simulations of scheme 2 in Fig. 6 are in conflict with the experimental results and that scheme 2 has to be amended. We have also modeled the equivalent of scheme 2 with desensitization from A_2R, and this produced the same conflicts with the experimental evidence.

The essential defect of scheme 2 is recovery from desensitization through A_2O. The only remedy is a circular reaction scheme containing a separate pathway for recovery. A circular reaction scheme already has been suggested by Katz and Thesleff (1957) and has been further developed by numerous authors, recently by Cachelin and Colquhoun (1989) and Dilger and Liu (1992). The circular scheme 3 seems to be sufficient to describe our results:

$$
\begin{array}{ccccccc}
& A & & A & & & \\
R & \underset{k_{-1}}{\overset{2k_1}{\rightleftharpoons}} & AR & \underset{2k_{-2}}{\overset{k_2}{\rightleftharpoons}} & A_2R & \underset{\alpha}{\overset{\beta}{\rightleftharpoons}} & A_2O \\
d_2 \updownarrow d_{-2} & & & & & & d_1 \nearrow \swarrow d_{-1} \\
D & \underset{k_{-3}}{\overset{2k_3}{\rightleftharpoons}} & AD & \underset{2k_{-4}}{\overset{k_4}{\rightleftharpoons}} & A_2D & &
\end{array}
\tag{3}
$$

10^{-4} M ACh   **outside-out patch, - 80 mV**

10 pA
100 ms

FIGURE 4   Three recordings of channel currents elicited by pulses of 10^{-4} M ACh in the same patch. To show the single channel currents more clearly, the outside-out patch was polarized to -80 mV, which is an unusually high polarization in the present investigation. Note the absence of channel openings after the ACh pulse has ended; in the first trace a burst of channel openings was finished after the end of the ACh pulse. Except for this type of completion of a burst, no channel openings were seen in the 50 pulse intervals of >1-s duration of this experiment.

In scheme 3 the rates $k_1 = k_2$, $k_{-1} = k_{-2}$, α and β are the same as those assumed in scheme 2. For a first simulation of the behavior of scheme 3, we take $d_1 = 20$ s^{-1} as before and chose $d_{-1} = 0.02$ s^{-1}, $d_2 = 0.214$ s^{-1}, $d_{-2} = 20$ s^{-1}, and $k_{-3} = k_{-4} = 4$ s^{-1}, as explained below. The other rate constants are irrelevant in the present context (see Table 1, set 2) and will be determined below.

Simulation of the double-pulse experiment with scheme 3 in Fig. 7 A results in an approximately correct time course of desensitization and of recovery from desensitization. The blowup of the end of the ACh pulse in Fig. 7 B shows a realistically low steady state of desensitization, $p_{0, ss}$ approaching 0.001, as determined by $d_{-1}/d_1 = 0.02/20 = 0.001$. After the end of the ACh pulse, at 400 ms, p_0 drops rapidly to zero. This occurs since $k_{-3} = k_{-4}$ and d_{-2} are much larger than d_{-1}, and the desensitized states empty toward R through the state D. After removal of ACh, essentially only the bursts, the oscillations between A_2R and A_2O continue until they are terminated with the rates $2k_{-2}$ and d_1; this process generates the rapid decay of p_0 after the termination of the ACh in Fig. 7 B. Scheme 3 thus avoids the two main shortcomings of scheme 2: the high value of

$p_{0, ss}$ and the reopenings of channels during recovery from desensitization.

The time course of recovery from desensitization calculated on the basis of scheme 3 has been included in Fig. 5. It can be seen that the simulation agrees very well with the measured curves. The time course of recovery is determined by the slowest steps in this direction in scheme 3, k_{-3} and k_{-4}. The value 4 s^{-1} gave an optimal fit. The back rate d_{-2} was chosen to be relatively high, at 20 s^{-1} (see Discussion), so d_{-2} does not limit the rate of recovery.

In the range of ACh concentrations in which recovery from desensitization can be measured readily, from 10^{-5} to 10^{-3} M ACh, the time courses of recovery were found to be little influenced by the ACh concentration during the pulse and also by pulse duration (experiments not shown here, see also Franke et al., 1992a). Simulations based on scheme 3 had the same result. In this range of ACh concentrations, the probabilities of the states R, O, and A_2D, p_R, p_0, and p_{A2D}, respectively, reach saturation levels quite rapidly during the ACh pulse (see Fig. 11), and therefore the conditions at the end of a pulse are
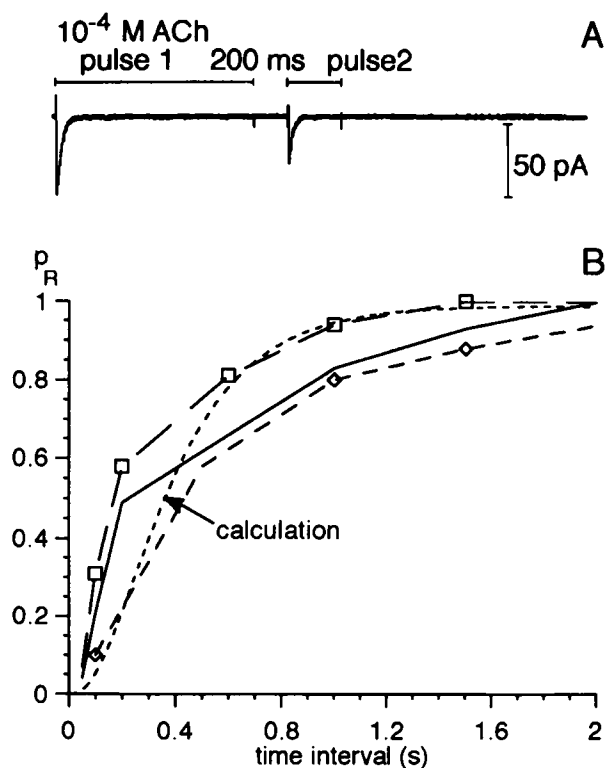
FIGURE 5 (A) Current response to two pulses of 10^{-4} M ACh, with a pulse interval of 200 ms. Average of 15 responses. $p_{o, max}$ elicited by pulse 2 divided by $p_{o, max}$ elicited by pulse 1 measures the extent of recovery from desensitization during the 200-ms pulse interval; this ratio is equivalent to the probability of the R state of the channel, p_R, after 200 ms of recovery from desensitization. p_R is plotted versus the pulse interval for two patches ($\square$ and $\Diamond$), whereas the short-dash curve is a simulation according to scheme 2 with set of parameters in Table 1.

little dependent on ACh concentration or pulse duration, unless extremely short pulses are given.

Desensitization in the absence of ACh (sleeping channels)

The circular scheme 3 necessarily has two pathways for desensitization, from A_2O and also from R. The desensitization from R, without binding of ACh, has two consequences. First, in the absence of ACh, a fraction d_2/d_{-2} of the channels will not be in the state R but in the desensitized state D. On application of ACh, these "sleeping" channels are not available immediately and contribute to the ACh response only after returning to R from D with the rate d_{-2}. Second, desensitization from R is most effective in the absence of ACh and declines with increasing ACh concentration when the R state becomes more and more improbable.

The fraction of sleeping channels in the absence of ACh, d_2/d_{-2}, can be estimated by determining $p_{o, max}$ achieved by application of a high ACh concentration, e.g., 10^{-4} M. With 10^{-4} M ACh, the first binding step has
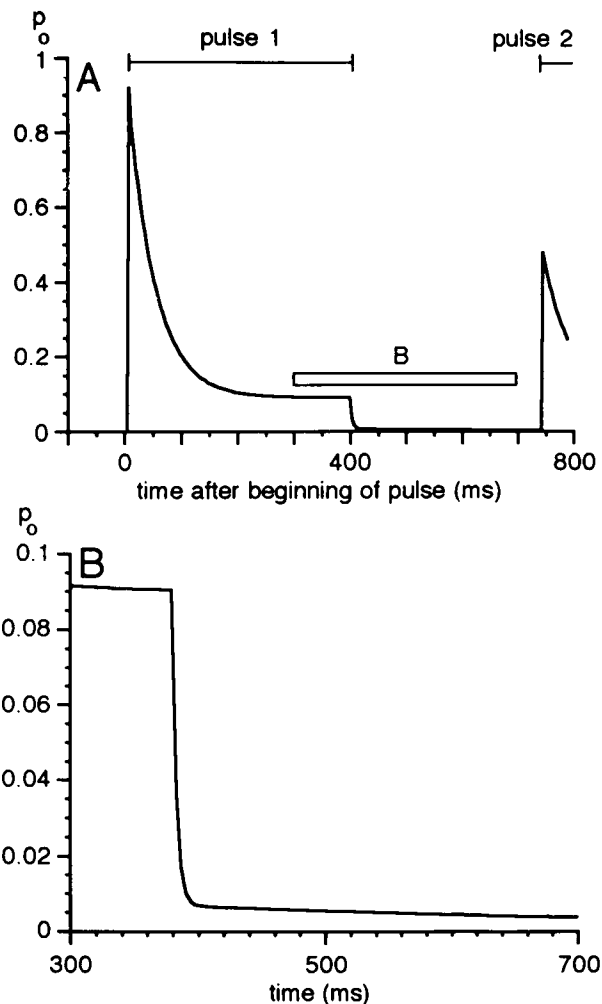
FIGURE 6 (A) Simulation of the time course of average channel opening, p_o, elicited by two pulses of 10^{-4} M ACh, modeling scheme 2. In B the time period from 300 to 700 ms (box in A) is shown, with higher resolutions in p_o and in time. The rate constants $k_1 = k_2 = 1.5 \times 10^8 \cdot M^{-1} s^{-1}$, $k_{-1} = k_{-2} = 8,000 s^{-1}$, $\alpha = 700 s^{-1}$, $\beta = 30,000 s^{-1}$, $d_1 = 20 s^{-1}$, and $d_{-1} = 2 s^{-1}$ were assumed.

a rate of 30,000 s^{-1} that is several orders larger than d_{-2}. $p_{o, max}$ therefore is limited by the fraction of sleeping channels. To obtain absolute values of $p_{o, max}$, the num-

TABLE 1 Rate constants in scheme 3

Constants	Set 1	Set 2	Set 3
$k_1 = k_2$	1.5×10^8 M^{-1} s^{-1}	Same	Same
$k_{-1} = k_{-2}$	8,000 s^{-1}	Same	Same
$k_3 = k_4$	1.5×10^8 M^{-1} s^{-1}	Same	Same
$k_{-3} = k_{-4}$	4 s^{-1}	Same	Same
α	700 s^{-1}	Same	Same
β	30,000 s^{-1}	Same	Same
d_1	20 s^{-1}	20 s^{-1}	100 s^{-1}
d_{-1}	0.2 s^{-1}	0.02 s^{-1}	0.1 s^{-1}
d_2	0.0214 s^{-1}	0.214 s^{-1}	0.214 s^{-1}
d_{-2}	20 s^{-1}	Same	Same

ber of channels opening in the peak response and also the number of activatable channels in the patch has to be compared. The number of channels in a patch can be determined if the probability of opening of a channel is high and the number of channels is low. This is obvious for patches containing only one channel, in which application of a pulse of high ACh concentration almost always elicits opening of one channel and never that of two channels. Fig. 8 shows an example for a patch containing two channels. In one of the 10 responses to pulses with 10^{-4} M ACh, only one channel opened at the peak response, and in 9 responses two channels opened simultaneously. If two activatable channels are assumed, then $p_{0, max}$ was 0.93. The distributions of probabilities in Fig. 8 demonstrate that in this and another experiment the numbers of double and single responses are distributed exactly like predicted by a binominal formula. On the other hand, simulation of the response of scheme 3 to a 10^{-4} M ACh pulse results in $p_{0, max} = 0.93$ (see responses to pulse 1 in Figs. 6 and 7; $p_{0, max}$ is reached before desensitization through d_2). The measured and the simulated $p_{0, max}$ thus agree exactly. Consequently, there is no evidence for sleeping channels, and all channels present are in the R state. d_2/d_{-2} therefore can be estimated to be smaller than 0.01.

Predesensitization by low ACh concentrations

Reaction scheme 3 contains binding reactions with ACh of the desensitized receptors/channels with very high affinity, $k_{-3}/k_3 = 2.7 \times 10^{-8}$ M (see Table 1). Such additional binding steps are necessary to achieve microscopic balance of the reactions; in a circular scheme, the products of the reaction rates in both directions have to be equal. The especially high affinity binding of ACh to the desensitized receptors is necessary to account for the desensitizing effects of low ACh concentrations, as first pointed out by Feltz and Trautmann (1982).

When, for instance, 10^{-6} M ACh were applied in the background in the superfusion to an outside-out patch, very little channel opening was elicited ($p_{0, ss} = 0.01$ to 0.001; see Fig. 10). A short test pulse of high concentration of ACh that was added to the background of 10^{-6} M ACh by the liquid filament switch elicited a full response immediately after switching on the background of 10^{-6} M ACh, but repeated test pulses brought successively smaller responses (Fig. 9 A). These responses declined with an approximate time constant of 2 s, in agreement with the time constant of desensitization reported in Franke et al. (1992b) (Fig. 1 B) for 10^{-6} M ACh. Finally, the response to the test pulse went down to 0.07 of the initial amplitude. Background superfusions with 10^{-5} M ACh suppressed the responses to test pulses completely, whereas 10^{-7} M ACh had very little predesensitizing effect (Fig. 9 B) (see also Franke et al., 1992a).

The dose-response curves for predesensitization are plotted in Fig. 9 B for two experiments. Simulated re-
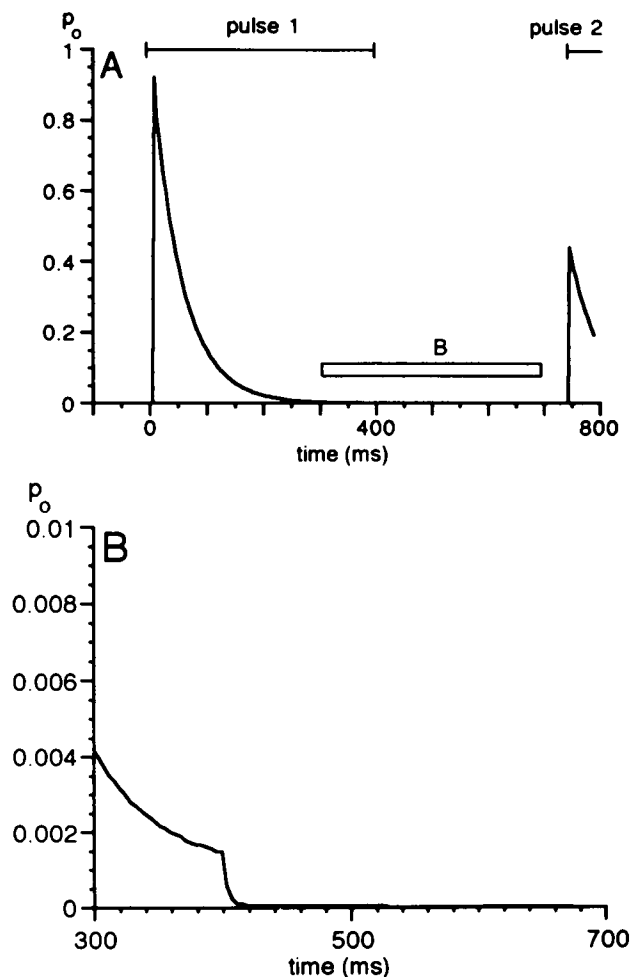

FIGURE 7   (A) Simulation of the time course of average channel opening, p_0, elicited by two pulses of 10^{-4} M ACh for the scheme 3. (B) Magnified response at the end of the first ACh pulse (box in A). Set 2 of rate constants in Table 1 was assumed.

sponses are also given that were calculated for the sets 1 and 2 of rate constants in Table 1. These sets differ only in the rate constant d_{-1}, which in relation to d_1 controls the equilibrium between A_2O and A_2D in scheme 3 (see next section). The level of this equilibrium shifts the calculated dose-response curve for predesensitization, and the measured responses, also those that were not plotted here, fit between the calculated curves. The steepness of the calculated curves depends on k_{-3}/k_3 and on k_{-4}/k_4 (compare Fig. 12). In reaction scheme 3 with the rates of Table 1, ACh concentrations between 10^{-7} and 10^{-5} M produce little channel opening, but eventually the channels will assume one of the desensitized states, predominantly through $A_2O \rightharpoonup A_2D$ but also through $R \rightharpoonup D$. Once in a D state, most of the channels will be caught in A_2D, since the forward rates in $D \rightharpoonup AD$ and $AD \rightharpoonup A_2D$ are much larger than the back rates. The channels in A_2D are not available for activation by an added high concentration pulse of ACh. These experiments incidentally exclude the possibility that the resen-
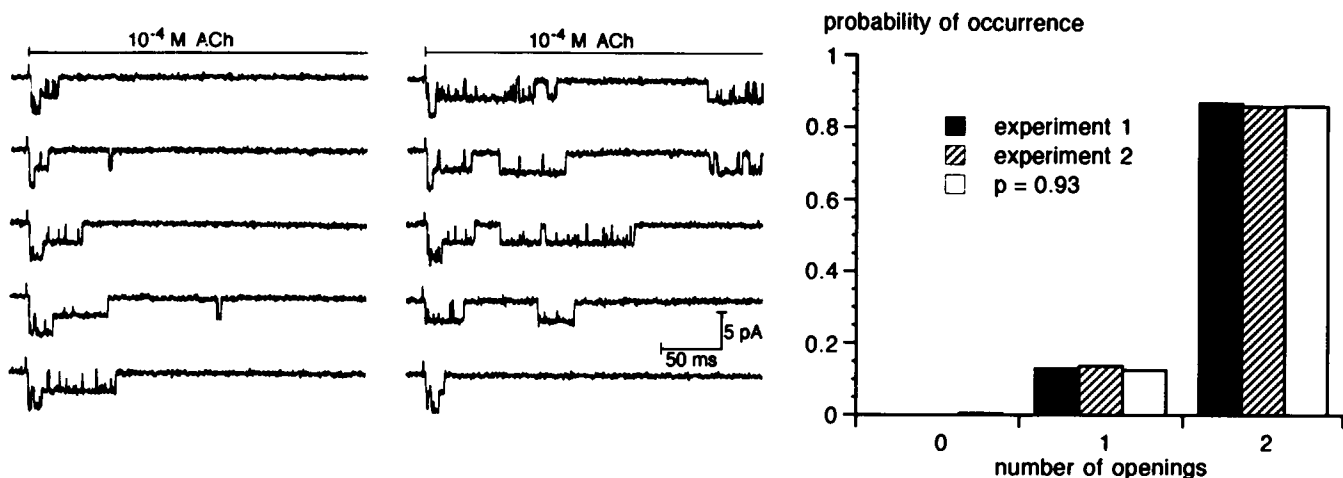
FIGURE 8 Ten single recordings of responses to 10^{-4} M ACh pulses in one patch that contained only two channels. The plot gives evaluations of the results of two experiments, with 104 and 128 recordings, respectively. The probabilities of occurrence of openings of 0 channels, 1 channel, and 2 channels after an ACh pulse are given. In addition, a binominal distribution with $n = 2$ states and a probability $P = 0.93$ is shown.

sitization/desensitization pathway goes from AD to AR instead of from D to R (scheme 3). Simulation of this reduced desensitization loop shows that the dependence of predesensitization is not steep enough and that recovery from desensitization is too slow.

The steady-state response to ACh

The last step in the reaction scheme 3 left to be discussed is the main desensitization step $A_2O \rightleftharpoons A_2D$. As discussed above, an alternative would be to assume that the desensitization reaction proceeds via $A_2R \rightleftharpoons A_2D$, with d_1 increased by a factor β/α. We will discuss only the first possibility, since the A_2O state is much more probable than the preceding A_2R, and at high ACh concentrations desensitization from A_2O proceeds nearly with the rate d_1, since $p_{o, max}$ is almost 1. The rate constant d_1, therefore, has to be approximately the reciprocal of τ_d at high ACh concentrations. The τ_d in different patches vary between 10 and 60 ms (Fig. 3), and consequently d_1 values of 20 s^{-1} to 100 s^{-1} have been selected (Table 1).

We have not yet discussed the dose-response curve for $p_{o, ss}$, the opening response in steady-state reactions with ACh (Fig. 10) (see also Franke et al., 1992b). $p_{o, ss}$ rose with increasing ACh concentration but reached a saturation level already with 10^{-6} M ACh. This dose-response curve for $p_{o, ss}$ may be compared with that for $p_{o, max}$ (Fig. 1), which reaches saturation above 10^{-4} M ACh and rises by two orders of magnitudes between 10^{-6} and 10^{-3} M ACh. Although the saturation level for $p_{o, max}$ was almost 1, for $p_{o, ss}$ this level was 0.01 to 0.001 in different patches (Fig. 10). The variation of the saturation level for $p_{o, ss}$ was not correlated with the variation in τ_d; relatively high $p_{o, ss}$ were associated both with low and high τ_d (see Fig. 5 of Franke et al., 1992b).

In the reaction scheme 3, $p_{o, ss}$ at high ACh concentrations is obviously given by the ratio d_{-1}/d_1. As discussed above, at high ACh concentrations, p_{A2D} approaches one

in the steady state, and $p_{o, ss} = (d_{-1}/d_1) p_{A2D}$ will be approximately equal to d_{-1}/d_1. Therefore, in the sets of rate constants for scheme 2 in Table 1, either $d_1/d_{-1} = 100$ or $d_1/d_{-1} = 1,000$ were selected, corresponding to $p_{o, ss}$ of 0.01 or 0.001, respectively. Calculated $p_{o, ss}$ are added in Fig. 10 for these two equilibria. The two calculated curves simulate the measured dose-responses quite well. Also, in the calculated $p_{o, ss}$, saturation is reached already with 10^{-6} M ACh. This reflects the high ACh affinity of the D states of the channel ($k_{-3}/k_3 = k_{-4}/k_4 = 2.7 \times 10^{-8}$ M) that drives most channels into the A_2D state on application of even a low ACh concentration.

The $p_{o, ss}$ in Fig. 7 are "steady-state values" measured at the end of pulses of 500-ms duration with 10^{-4} M ACh or in pulses of 10-s duration with 10^{-6} M ACh. These pulse durations correspond to $\sim 10 \times \tau_d$, which should be sufficient to reach the steady-state level. However, when ACh was applied for many minutes, the average channel opening was often found to be ~ 10 times lower than the $p_{o, ss}$ measured at the end of a 0.5-s pulse. For instance, in the experiment of Fig. 13, $p_{o, ss}$ was 0.04 at the end of a pulse of 10^{-4} M ACh of 430-ms duration, which is an unusually high $p_{o, ss}$ value. In the continuous superfusion of 10^{-4} M ACh that followed the pulse experiment, the $p_{o, ss}$ was 0.001. It seems, therefore, that there is a slow component of desensitization that has a very low amplitude. This slow component cannot be in series with the rapid one, since recovery from desensitization is much faster than the slow desensitization and independent from the duration of application of ACh. The only scheme compatible with the data is a second desensitization loop in scheme 3, which starts from A_2O and goes to $A_2D_s \rightleftharpoons AD_s \rightleftharpoons D_s \rightleftharpoons R$, with $d_{1,s} < 1$ s^{-1} and $d_{-1,s}/d_{1,s} > 1,000$ (the other rate constants like in Table 1). After reaching a first equilibrium determined by d_1/d_{-1}, in a very long ACh application the channels will shift slowly to the lower $p_{o, ss}$ determined by $d_{1,s}/d_{-1,s}$.
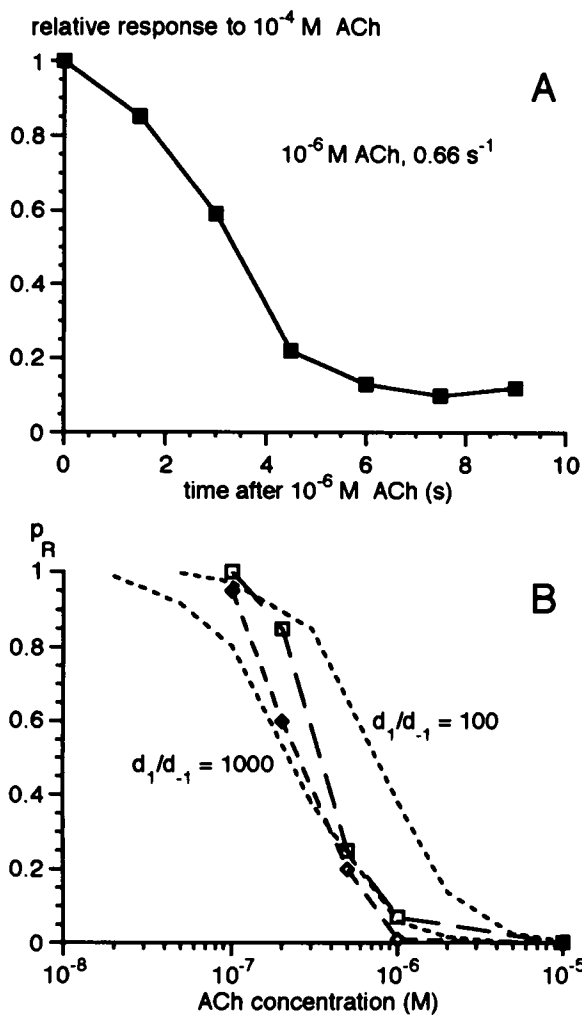
FIGURE 9 Predesensitization by low ACh concentrations that were present continuously. (A) Ordinate relative amplitudes of $p_{o, \max}$ elicited by pulses of 10^{-4} M ACh was added to the background superfusion. (B) Reduction of the $p_{o, \max}$ that was elicited by a 10^{-4} M pulse of ACh by the continuous, background ACh concentration (absissa), in relation to $p_{o, \max}$ without predesensitization (ordinate). These values correspond to p_R, the probability of the nonliganded receptor. Experimental results from two patches (each point based on ≥10 recordings), and simulated curves according to reaction scheme 2, using set 1 ($d_1/d_{-1} = 100$) or set 2 ($d_1/d_{-1} = 1,000$) of rate constants in Table 1.

The time course of this process cannot be determined well with the relatively low numbers of channels present in a patch.

The complete circular reaction scheme 3

We have determined most of the rate constants in scheme 3 by experimental protocols relating more or less directly to the different reaction steps. $k_1 = k_2$, α and β are based on the analysis of single channel kinetics (see Colquhoun and Sakman, 1985) and of the peaks and rising phase of responses to pulses of different ACh concentrations (Franke et al., 1991b). d_1 can be derived

from τ_d and d_1/d_{-1} from $p_{o, ss}$. $k_{-3} = k_{-4}$ are determined from the time constant of recovery from desensitization and k_{-3}/k_{+3} by the high affinity of binding of ACh to the D states, which is necessary for a steep dose-response to predesensitizing low ACh concentrations but also for saturation of the $p_{o, ss}$ dose-response with $>10^{-6}$ M ACh. d_{-2} has to be much larger than $k_{-3} = k_{-4} = 4\ \text{s}^{-1}$ in order not to limit the rate of recovery from desensitization. d_2/d_{-2} should be smaller than 0.01 to limit the proportion of "sleeping channels" in absence of ACh to an insignificant value. With these limitations, $d_{-2} = 20\ \text{s}^{-1}$ was chosen, and the exact value of d_2 was calculated to comply with the rule of balance of reaction rates in circular schemes. Larger values than $20\ \text{s}^{-1}$ could have been selected for d_{-2}, with a proportional increase in d_2. An upper limit for d_2 is given by the time course of desensitization on applying 10^{-6} M ACh. The τ_d with 10^{-6} M ACh was 1–2 s (Fig. 9 A) (Franke et al., 1992b, Fig. 1 B). Desensitization via $A_2O \rightleftharpoons A_2D$ generates just this time course (Fig. 2 B). Therefore, the contribution of desensitization from R must be negligible with 10^{-6} M ACh. Consequently, $d_2 \ll 300\ \text{s}^{-1}$, the latter being the rate of the $R \rightleftharpoons AR$ reaction with 10^{-6} M ACh. This possible scaling factor for d_2 and d_{-2} of ~ 100 is the only free choice in the sets of reaction rates (Table 1).

The dose-responses of $p_{o, \max}$ and of $p_{o, ss}$ predicted by reaction scheme 3 have been plotted in Fig. 2 and in Fig. 10, respectively. The time courses of the occupancies of the R, A_2O, and A_2D states, during and after an ACh pulse, are plotted in Fig. 11. The upper graphs show the results of a 10.5-s pulse with 10^{-6} M ACh. The dominant effect during the pulse is a symmetrical fall in R and rise in A_2D, with a time constant of ~ 2.3 s. The sum of p_R and p_{A2D} is almost 1, the other states in scheme 3 being quite improbable. To plot the time course of the open
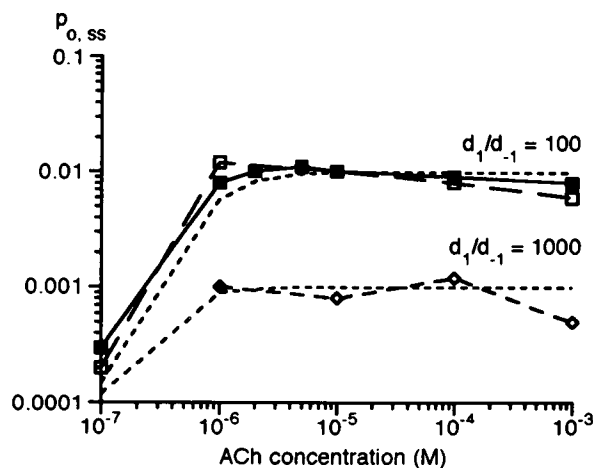

FIGURE 10 Probability of the open state at the end of a long ACh pulse, $p_{o, ss}$, (ordinate) versus the ACh concentration during the pulse (abscissae). Results from three patches (□, ■, and ◇) and dashed curves from simulation of scheme 2 with the rate constants of set 1 ($d_1/d_{-1} = 100$) or of set 2 ($d_1/d_{-1} = 1,000$) of Table 1.

10⁻⁶ M ACh

10⁻⁶ M ACh

A₂D

R

A₂O

time (s)

A₂O

time (s)

10⁻⁴ M ACh

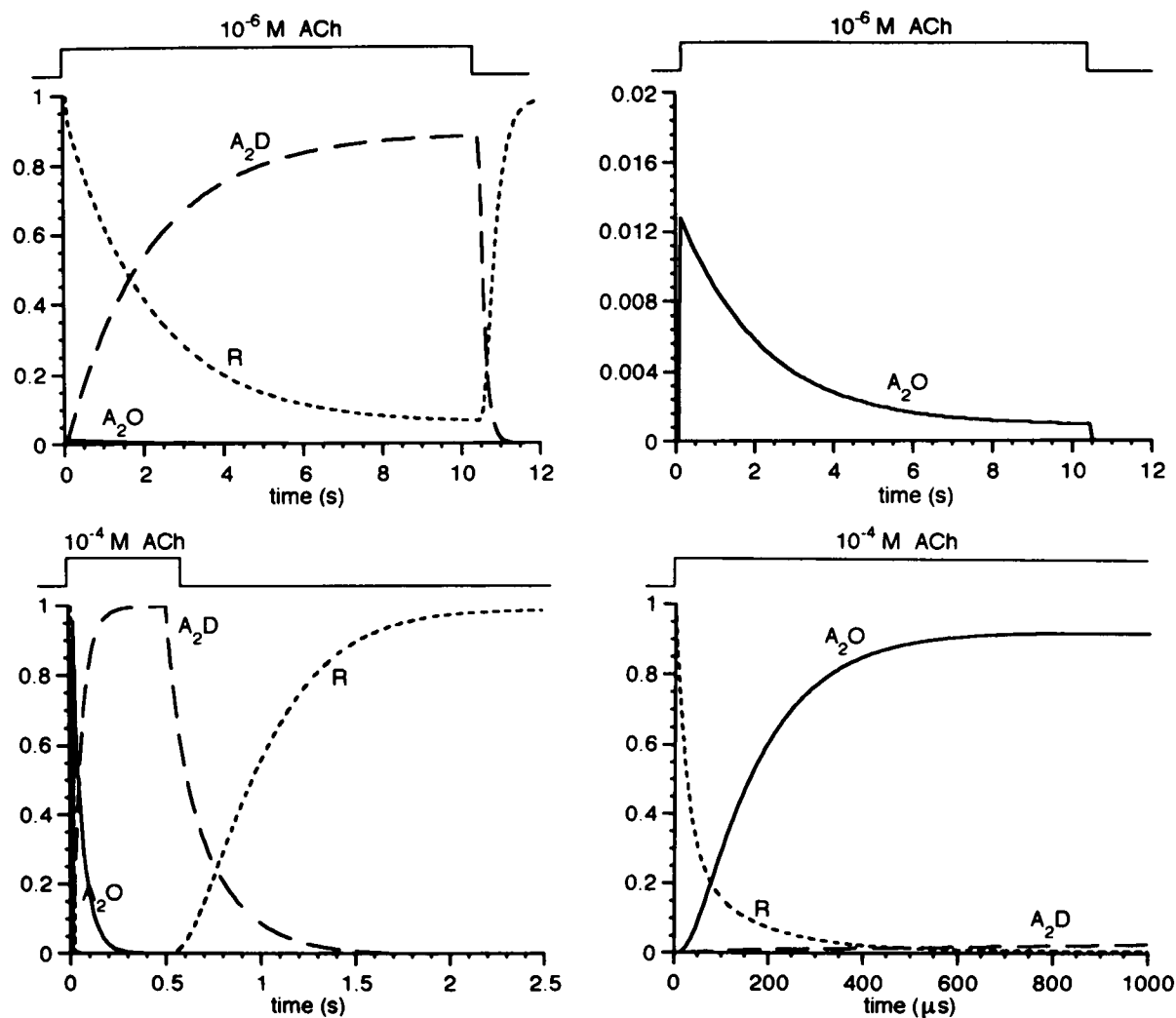10⁻⁴ M ACh

A₂D

R

A₂O

time (s)

A₂O

R

A₂D

time (μs)

FIGURE 11   Simulations of time courses of the probabilities of the states R, A_2O, and A_2D in scheme 2 (ordinates) during and after a 10-s pulse of 10^{-6} M ACh (*upper graphs*) or a 0.6-s pulse of 10^{-4} M ACh (*lower graphs*). The complete graphs are the ones to the left; to the right, either the ordinate or the time scales are magnified.

state, A_2O, the ordinate had to be amplified 50 times (upper right plot in Fig. 11). $p_{o,\,max}$ is 0.013, and opening declines to $p_{o,\,ss}$ of 0.001 with τ_d = 2.3 s, which was also the time constant of the changes in R and A_2D. After the ACh pulse, R returns to 1 and A_2D to zero with a time constant of ~0.4 ms, and channel opening stops.

In the lower graphs of Fig. 11, a 0.5-s pulse with 10^{-4} M ACh was assumed. Such a pulse empties the R state very rapidly, p_R = 0.1 being reached within <200 μs. Channel opening increases more slowly; p_o = 0.9 is reached only after 550 μs. In comparison to the rapid changes in R and A_2O, the desensitized state A_2D is filled much more slowly, with a time constant τ_d = 54 ms. About 200 ms after application of ACh, almost all channels are in the A_2D state. When ACh is washed off, channel opening stops, and the R state is refilled from A_2D with a time constant of approximately 0.4 s. This refilling of the R state corresponds to recovery from desensitization.

The time constant of desensitization in excised and cell-attached patches

In our studies on nicotinic receptors on mouse muscle and also in those of Dilger and Brett (1990) and Dilger and Liu (1992) on nicotinic receptors on clonal mammalian muscle cells (BC3H cells), isolated outside-out patches were exposed to rapid changes in ACh concentrations and time constants of desensitization from 10 to 100 ms were observed for high ACh concentrations. These time constants are much shorter than those obtained by ACh superfusion of muscle fibers, which were in the range of seconds to minutes (see Cachelin and Colquhoun, 1989). It might be argued that the short time constants measured in outside-out patches reflect an altered condition of the patches, for instance, due to changes in the "intracellular" milieu. It is not feasible to disprove this possibility directly, because sufficiently rapid concentration changes cannot be performed within the tip of a cell-attached patch, in which case the

intracellular milieu would be normal. An indirect approach has to be used. When high ACh concentrations are applied, in the steady state the primary bursts of channel openings are grouped in "clusters," which are groups of bursts of channel opening separated by relatively long closed periods. At an ACh concentration of 10^{-3} M, for example, the rates $R \rightleftharpoons AR$ and $AR \rightleftharpoons A_2R$ are $>10^5$ s^{-1} and the states R and AR have extremely short lifetimes. Therefore, the channels flicker practically between A_2R and A_2O. The flickering activity is interrupted by long closed periods (>10 ms), which define the clusters. The long closed periods are generated by desensitization. The average duration of clusters at a certain ACh concentration therefore should be equal to the time constant of desensitization at the respective ACh concentration as could be concluded from Colquhoun and Hawkes (1982) and Colquhoun and Ogden (1988).

The stochastic opening and closing behavior of a channel as predicted by the reaction scheme 3 was simulated by a computer program, and examples are shown in Fig. 12 A. Clusters were defined as periods in which closed times between channel openings were >10 ms, and the durations of such clusters were evaluated. The distribution of cluster lengths in Fig. 12 B can be fitted by a time constant $\tau_c = 53.3$ ms. In the simulation of Fig. 12 A, desensitization rate d_1 20 s^{-1} was assumed, which due to the maximal p_0 at 10^{-4} M ACh of 0.94 generates a time constant of desensitization $\tau_d = 53.2$ ms (Fig. 12 C). This demonstrates that in the model of scheme 3 the average duration of the clusters is equal to the time constant of desensitization.

The same equality of time constants can be shown also for outside-out patches (Fig. 13). The upper recording is average clamp current elicited by a pulse of 10^{-4} M ACh. The time constant of desensitization of this response was $\tau_d = 46$ ms. After the pulses of ACh, the patch was continuously exposed to 10^{-4} M ACh, and steady-state responses of the largely desensitized channels were recorded. The clusters of openings had an average duration of 48 ms, which agrees well with the time constant of desensitization. This agreement of the time constant of desensitization and of the mean cluster length was seen in all experiments of this type ($n = 5$), in which ACh concentrations of 10^{-3} M and of 5×10^{-5} M were also used.

We have shown now for the reaction scheme 3 and for the outside-out patches that the time constant of desensitization and the average duration of clusters are equivalent. The average duration of clusters can be measured also in cell-attached patches, with a constant ACh concentration in the patch pipette that elicits a steady-state response (Fig. 14). The clusters of openings in these recordings look very similar to those in Fig. 13 that were obtained in outside-out patches. The distribution of cluster lengths in Fig. 14 is fitted by an exponential with a time constant of 47 ms. This cluster length is in the

same range as those obtained in outside-out patches, and this was also true for other experiments of this type ($\tau_c = 32–74$ ms; $n = 6$). It has been shown above that τ_c and τ_d are equivalent. It may be concluded, therefore, that the rates of desensitization in cell-attached and in outside-out patches of embryonic like mouse muscles are in the same range. There is no evidence for a strong effect of the presence or absence of the normal intracellular milieu at the channels on their desensitization characteristics. The short time constants of desensitization of nicotinic receptors-channels measured by us and by Dilger and Brett (1990) and Dilger and Liu (1992) thus seem to be characteristics of the normal channel.

There are some indications for slight effects of removal of patches from the cell membrane. As also seen by Dilger and Liu (1992), occasionally the τ_d decreased slowly when tested by repetitive ACh pulses during the first minutes after excision of a patch. This decrease of τ_d was never more than by a factor of 2.

DISCUSSION

The reaction model of the embryonic receptor

We have based the analysis of the starting point of desensitization on recorded dose-response curves for the peak of channel opening elicited by a pulse of ACh, $p_{0,\,max}$, and for the time constant of the onset of desensitization, τ_d (Fig. 1). The theoretical starting point was the model of channel opening (scheme 1) as proposed by Colquhoun and Sakman (1985), which was shown to be applicable to the embryonic-like mouse-muscle channels by Franke et al. (1991b). Desensitization could start from any of the four channel states in this model. It might be produced by binding of ACh or may occur as a spontaneous conformation change. Desensitization without binding of ACh and starting from the open state A_2O (Fig. 2, A and D) was found to allow a complete description of the dose-response curves in Fig. 1. Alternatively, desensitization could also start from A_2R. Since the channel oscillates between A_2R and A_2O very rapidly and this oscillation is independent of concentration, these two states are practically indistinguishable for a comparatively slow process like desensitization. The model of scheme 2, however, is only sufficient to describe the dose-responses of Fig. 1. When data on recovery from desensitization are included, a number of further steps have to be added. But these further steps do not impair the validity of the model 2 for the description of the dose-response curves.

Compared with the simple linear desensitization scheme 2, the circular reaction (scheme 3) is much more complicated. However, only the circular model was able to cover three important characteristics of the channels. (a) After washout of ACh, only bursts of openings that started in presence of ACh were completed; there were
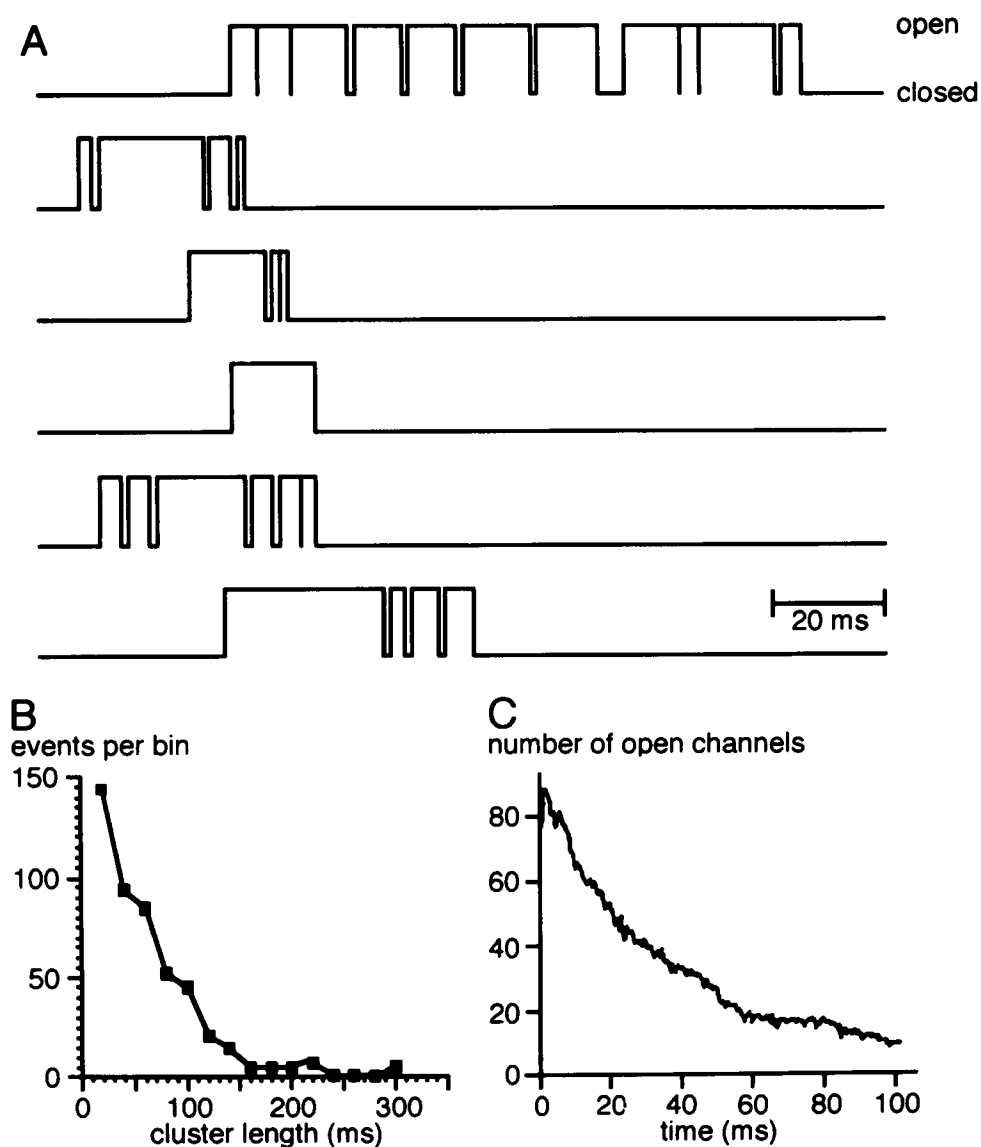
FIGURE 12 (*A*) samples of the simulated opening behavior of one channel in the presence of 10^{-4} M ACh in the steady state. The mean cluster length was 55.7 ms. A "circular" extension of the reaction scheme in Fig. 4 was assumed (scheme 2 in Franke et al., 1992a), with $d_1 = 20$ s^{-1} and $d_2 = 0.02$ s^{-1}. (*B*) Distribution of cluster length from simulated channel behavior in *A*. (*C*) Decay of simulated average opening of 100 channels after a pulse of 10^{-4} M ACh; τ_d of this decay was 53.3 ms.

no late openings during recovery from desensitization. (*b*) The values of τ_d, $p_{o, ss}$, and the time of half recovery could vary independently. (*c*) The dose-response curves for $p_{o, max}$ and for $p_{o, ss}$ were different, the desensitized receptors having a much higher affinity for ACh than the nondesensitized ones. The high affinity of the *D* states for ACh also is responsible for the almost complete desensitization of the channels by $>10^{-6}$ M ACh, whereas 10^{-6} M ACh elicited very little channel opening. The effect of predesensitization by low ACh concentrations and its relation to the high ACh affinity of the *D* states has been noticed already by Feltz and Trautmann (1982). A high affinity of the desensitized ACh receptor of 3 nM to 1 μM has been observed also in chemical binding studies (for review, see Ochoa et al., 1989). Sine and Taylor (1982) found k_D values for the binding of

Carbamylcholine to the nondesensitized and desensitized receptors (BC3H-cells) of 60 and 200 μM, respectively, which may be compared with our values of 53 μM and 27 nM. They estimated the proportion of sleeping channels, d_2/d_2, as 10^{-4}, whereas we obtained upper limits of this proportion of 1/100.

Dilger and Liu (1992) have obtained results on desensitization and resensitization in outside-out patches of BCH cell membranes that were very similar to ours, although they did not report the predesensitization by low ACh concentrations (Fig. 9). Dilger and Liu (1992) gave a general scheme to describe their results (Fig. 15). This scheme includes a blocked state A_2R^*A that corresponds to intermittent blocking of the channel by high ACh concentrations (see Sine and Steinbach, 1984, 1987). We have not included these features into scheme
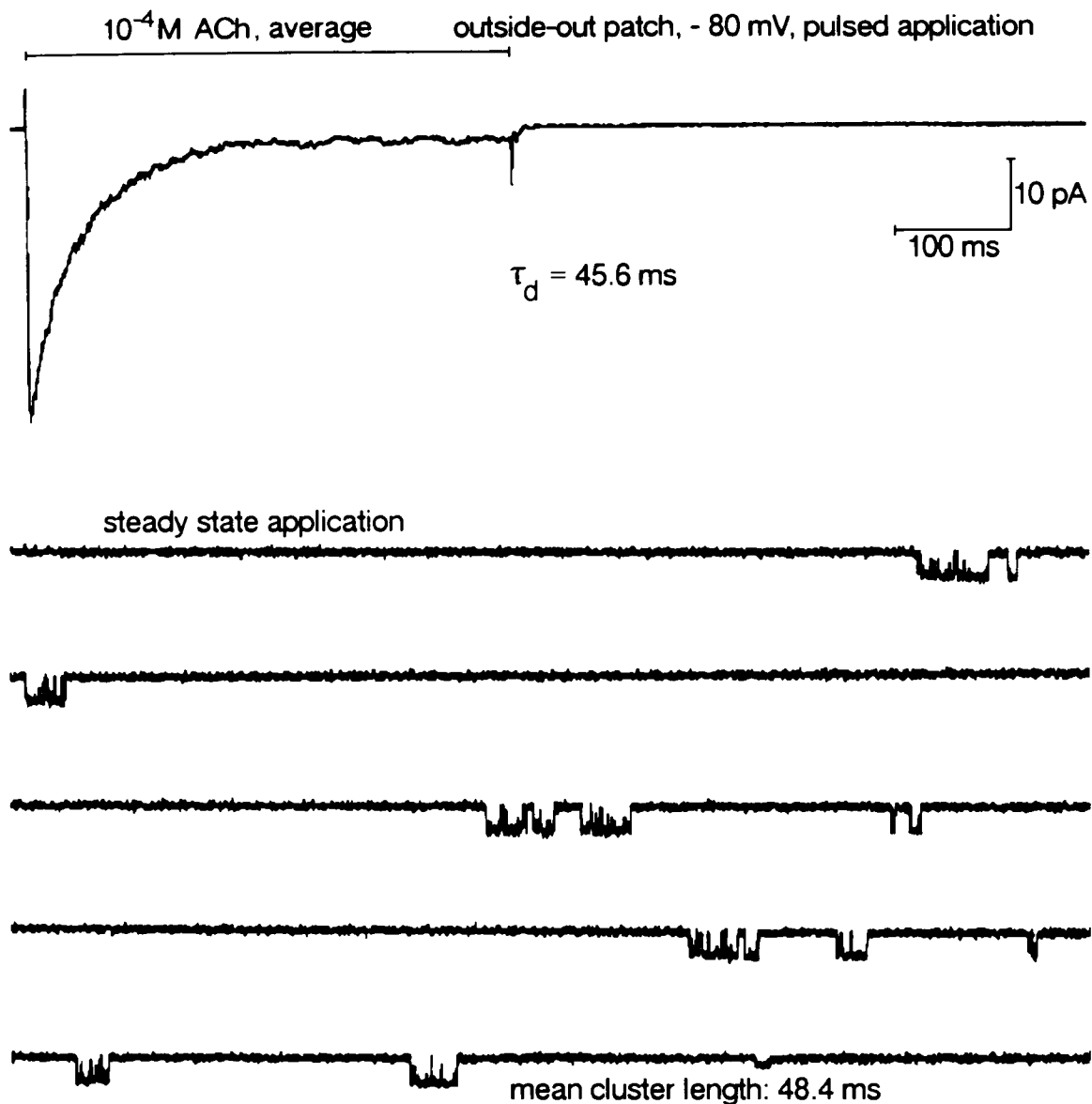
10⁻⁴M ACh, average   outside-out patch, - 80 mV, pulsed application

10^{-4} M ACh, average   outside-out patch, - 80 mV, pulsed application

τ_d = 45.6 ms

10 pA

100 ms

steady state application

mean cluster length: 48.4 ms

FIGURE 13 (*Upper*) Average current elicited by 18 pulses of 10^{-4} M ACh, time constant of desensitization τ_d = 45.6 ms. (*Lower*) Traces of current measured in the same outside-out patch during the steady-state superfusion of 10^{-4} M ACh, with a mean cluster length of 48.4 ms.

3 since at the potentials > −70 mV and concentrations ≤ 10^{-3} M, this channel block did not occur in our preparation. The scheme in Fig. 15 in addition contains desensitization reactions from all of the nondesensitized channel states, whereas in our model 3 there is only one effective route of desensitization, $A_2O \rightleftharpoons A_2D$. Dilger and Liu (1992) did not simulate the behavior of their reaction scheme, and therefore they could not see all the consequences of their assumptions. We have done the simulations (Fig. 15, *A–C*; using their upper limits of rate constants) mainly to demonstrate the predictions of a scheme that is not too different from our scheme 3. We simulated the scheme, including the blocked A_2R^*A state or not, which did not affect the results appreciably. The simulated dose-response curves for $p_{o, max}$ and $p_{o, ss}$

in Fig. 15 *A* agree approximately with the experimental results. Also, recovery from desensitization is simulated satisfactorily (not illustrated). However, the simulated dose-response curve for τ_d gives a too weak dependence on ACh concentration. Dilger and Liu (1992) found experimentally $1/\tau_d$ to be proportional to $p_{o, max}$ as we did (Fig. 1). The simulation of their model results in a curved relationship (Fig. 15 *B*) and in a τ_d at high ACh concentrations of only 15 ms, instead of their measurement of 60 ms. This discrepancy in τ_d seems to be due to the multiple pathways of desensitization in the scheme of Fig. 15 (see the discussion above on desensitization without binding from *R* and *AR*). Fig. 15 *C* plots the predicted effect of predesensitization at steady state on the reaction to large ACh pulses, i.e., on the probability

cell-attached, 10^{-3} M ACh, resting potential

2 pA

100 ms

47 ms

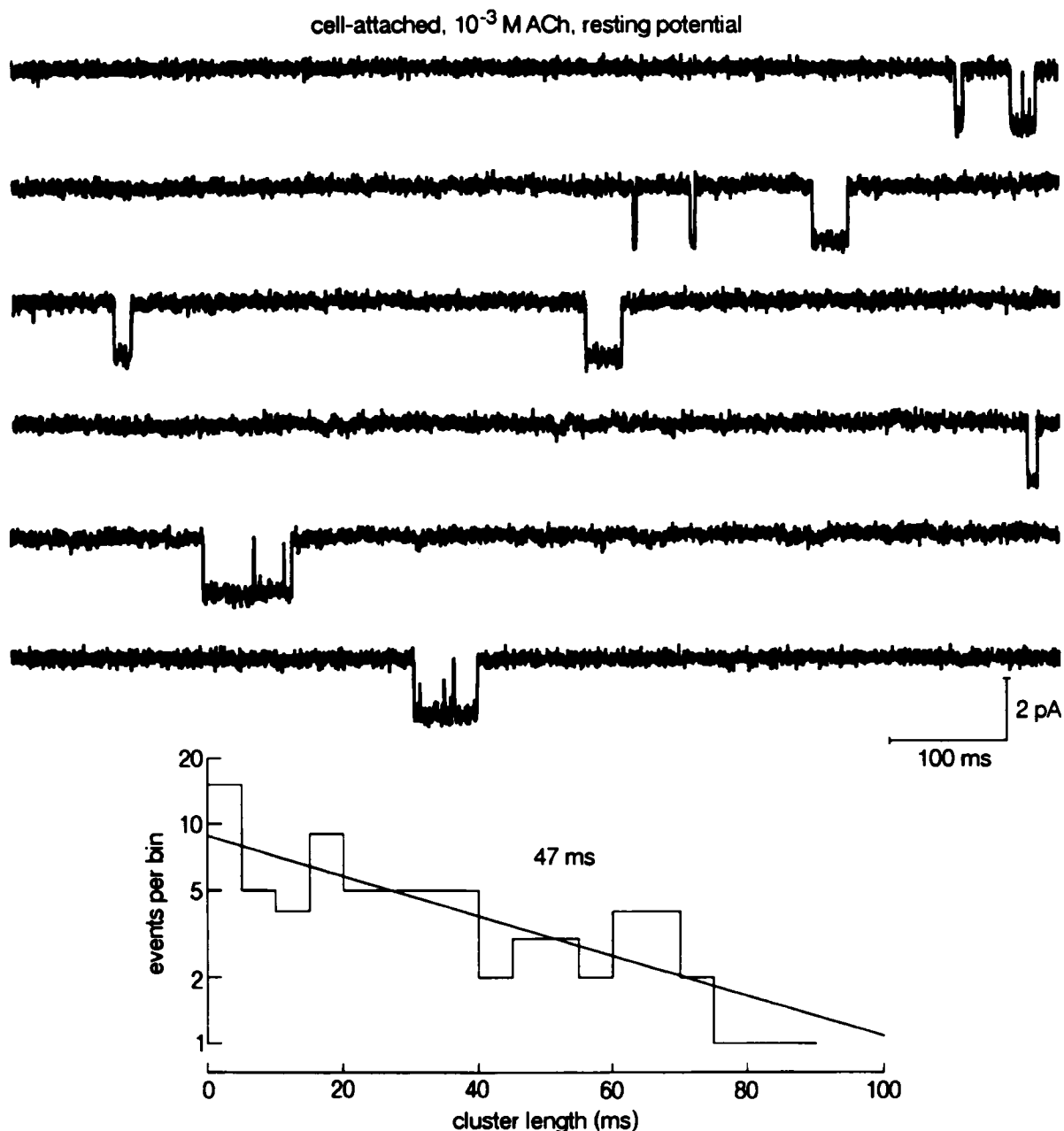events per bin — cluster length (ms)

FIGURE 14   Cell-attached patch-clamp recording with 10^{-3} M ACh contained in the pipette. The distribution of the lengths of clusters of openings (openings separated by closed periods > 10 ms) corresponds to an average cluster length of 47 ms (73 clusters evaluated).

of R. Dilger and Liu did not measure predesensitization, but their prediction could be compared with our experimental results in Fig. 9 B. The observed relation between ACh concentration and p_R is steeper and shifted to the left in comparison to Fig. 15 C. The main reason for this difference is the 100× lower affinity of the D states in the model of Fig. 15 as compared with the affinities assumed by us (Table 1).

A consistent finding in the ACh-ergic, but also in the glutamatergic channels (Dudel et al., 1990b, c), is the variability of the τ_d measured in different patches from the same muscle (see Fig. 3). The different τ_d could be

due to posttranslational modifications (Fiekers et al., 1987; Huganir and Greengard, 1987; Miles et al., 1987; Schuetze and Role, 1987; Caratsch and Eusebi, 1990). Remarkably, in one patch there was always only one value of τ_d. The influences that generate the different τ_d must be uniform on the scale of a single patch. On the other hand, when recording from a whole endplate, a mixture of "local" τ_d values should be effective.

The adult nicotinic receptor

Adult receptors have steeper dose-response curves for ACh than embryonic ones, and the channel opening

A 4×10^8 $M^{-1}s^{-1}$ A 2×10^8 $M^{-1}s^{-1}$ A 4×10^7 $M^{-1}s^{-1}$

$R \underset{20000\ s^{-1}}{\overset{}{\rightleftarrows}} AR \underset{40000\ s^{-1}}{\overset{}{\rightleftarrows}} A_2R \underset{500\ s^{-1}}{\overset{30000\ s^{-1}}{\rightleftarrows}} A_2R^* \underset{200000\ s^{-1}}{\overset{}{\rightleftarrows}} A_2R^*A$

$3\ s^{-1}\ |\ 0.3\ s^{-1}$ $60\ s^{-1}\ |\ 200\ s^{-1}$ $30\ s^{-1}\ |\ 3000\ s^{-1}$ $0.2\ s^{-1}\ |\ 20\ s^{-1}$ $0.2\ s^{-1}\ |\ 20\ s^{-1}$

A 4×10^8 $M^{-1}s^{-1}$ A 2×10^8 $M^{-1}s^{-1}$ A 4×10^7 $M^{-1}s^{-1}$

$D \underset{630\ s^{-1}}{\overset{}{\rightleftarrows}} AD \underset{1260\ s^{-1}}{\overset{}{\rightleftarrows}} A_2D \underset{500\ s^{-1}}{\overset{30000\ s^{-1}}{\rightleftarrows}} A_2D^* \underset{200000\ s^{-1}}{\overset{}{\rightleftarrows}} A_2D^*A$

A — without block, with block, $p_{o,\ max}$, $p_{o,\ ss}$; ACh concentration (M), axis 10^{-7} 10^{-6} 10^{-5} 10^{-4} 10^{-3}; y-axis 1, 0.1, 0.01, 0.001, 0.0001, 0.00001

B — $1/\tau_d\ (s^{-1})$, y-axis 70 60 50 40 30 20 10 0 -10; x-axis $p_{o,\ max}$ 0 0.2 0.4 0.6 0.8

C — $p_{R,\ ss}$, y-axis 1 0.8 0.6 0.4 0.2 0; x-axis ACh concentration (M) 10^{-7} 10^{-6} 10^{-5}
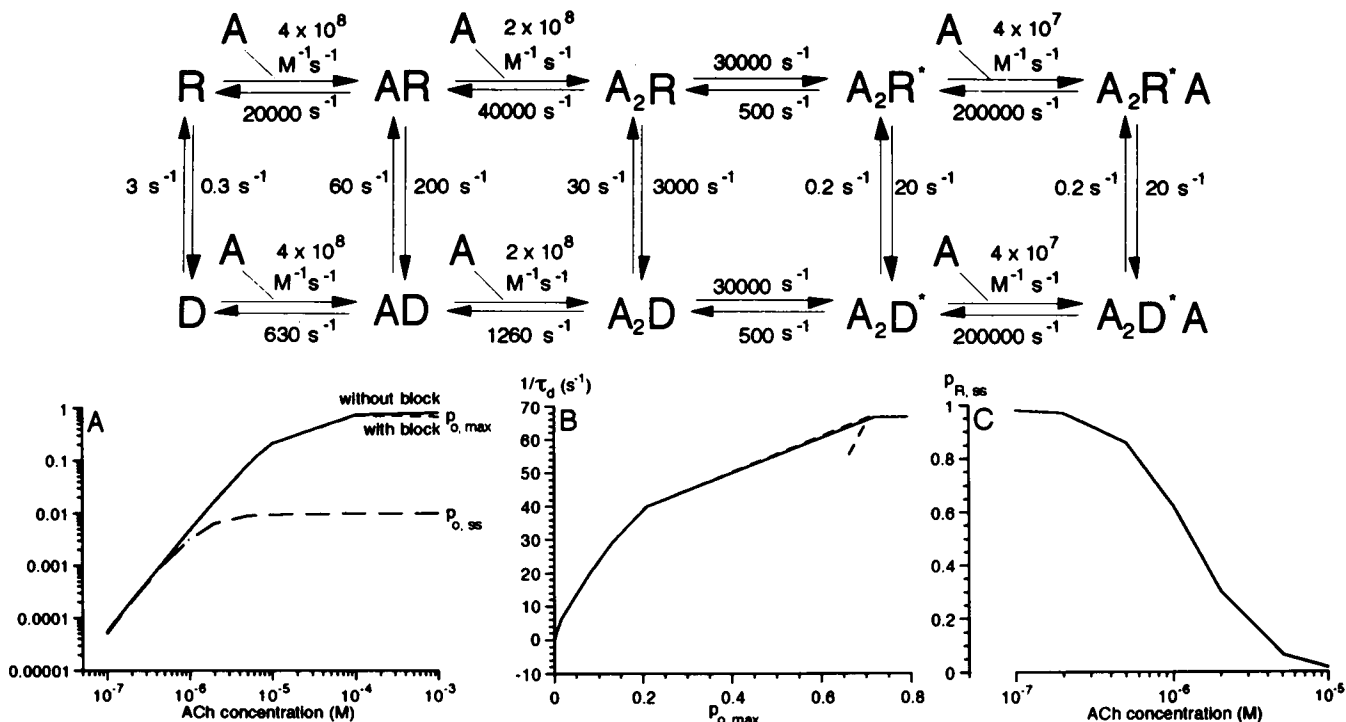
FIGURE 15   Reaction scheme suggested by Dilger and Liu (1992). A_2R^* is the open channel state, and A_2R^*A is a blocked state ("open channel block"). The plots are simulations of (A) the dose responses for $p_{o,\ max}$ and $p_{o,\ ss}$, (B) $1/\tau_d$ versus $p_{o,\ max}$, and (C) the dose-response for p_R, found as in Fig. 6. The simulations were done with and without the blocking step $A_2R^* \cdot A_2R^*A$, with very small effects for $p_{o,\ max}$ and a curious "hysteresis" for the simulation with block in B.

seems to require at least three binding steps for ACh (Franke et al., 1991a, b). $p_{o,\ ss}$ is even lower than in embryonic channels (Franke et al., 1992b). On the other hand, the dose-response relations for τ_d are almost the same in both channel types, including the range of variation of τ_d, and desensitization was monexponential. We did not yet test a quantitative model for the adult channels, but such a model should be essentially an extension of scheme 3.

High affinity binding to desensitized states

An obvious consequence of the high affinity of the desensitized states is a block of transmission when low ACh concentrations are present continuously, which in the adult system is prevented by the action of ACh-esterase but which may be important in case of block or absence of this esterase.

ACh binding to desensitized states also has been discussed in relation to posttetanic potentiation. Postsynaptic potentation (for reviews, see Magazanik, 1989; Scuka and Mozrzymas, 1992) was seen in the context of desensitization experiments already by Katz and Thesleff (1957) and may be discussed using scheme 3. Two ACh pulses of low concentration, given simultaneously to the same site, will result in a more than double as high a response than that to a single pulse, if the sum of the ACh concentrations at the receptors corresponds to a region

of the dose-response of $p_{o,\ max}$, in which the double-logarithmic slope is >1. If the response to ACh pulses is to be potentiated by the continuous presence of a conditioning low ACh concentration (Feltz and Trautmann, 1980, 1982), then steady-state desensitization limits this conditioning concentration to $<2 \times 10^{-7}$ M. With a conditioning ACh concentration of 2×10^{-7} M, half of the channels are desensitized (Fig. 9). An added 2×10^{-7} M ACh pulse will have a less than four times higher opening effect on the remaining channels than the 2×10^{-7} M pulse would have without conditioning. But since only half of the channels are activatable, the absolute opening effect of the "doubled ACh concentration" is less than two times that of the 2×10^{-7} M ACh pulse above. This kind of potentiation thus is limited to very low conditioning ACh concentrations.

Under some potentiating conditions (block of ACh-esterase, high quantum content of endplate currents), the decay of end-plate currents is slowed (Feltz and Trautmann, 1980; Ruzzier and Scuka, 1985, 1986). Magazanik et al. (1984) and Magazanik (1989) suggested that the complex AR might be a "silent source" of ACh after the released ACh is cleared from the synaptic cleft and might prolong synaptic currents. p_{AR} according to scheme 3 is always small, and after removal of ACh AR dissociates with a time constant of ~ 0.1 ms. However, if any application of ACh to the receptors is long enough to allow filling of the A_2D state, after removal of ACh disso-

ciation of the A_2D and the AD states will proceed with rates of 8/s and 4/s, respectively. ACh from this source might be rebound to the receptors and add some tail to the synaptic current. According to Fig. 9, $p_{A2D} = 0.5$ is reached after $\sim$2 s with 10^{-6} M ACh and after $\sim$40 ms with 10^{-4} M ACh.

Apparent discrepancy between desensitization in excised and cell-attached patches

In outside-out patches, we have reported time constants of desensitization, τ_d, of 10–60 ms, which are similar to those of Dilger and Brett (1990) and Dilger and Liu (1992) obtained also with outside-out patches, but from BCH cells. The onset of desensitization found on application of ACh to intact muscle fibres was much slower than observed in excised patches, with time constants of seconds to minutes (Katz and Thesleff, 1957; Feltz and Trautmann, 1982; Cachelin and Colquhoun, 1989). The two latter studies also showed two time constants of desensitization. Two principal explanations may be given for this difference in the behavior of channels in excised patches and channels in the intact muscle. (a) The excised patches present a nonphysiological state of the channels, which may be due for instance to the artificial medium at the "interior" side of the patch. (b) Application of ACh to endplates on intact muscles may be too slow and inhomogeneous to produce the concentration jumps required for rapid activation and desensitization of the channels.

A line of evidence was given in Figs. 12–14 that intends to show that desensitization of the channels in outside-out patches proceeds with the same rates as in patches of intact muscle membrane, i.e., in cell-attached patch-clamp recordings. This was done by establishing first that in the outside-out patches and in the simulation of the reaction scheme, the average duration of clusters of channel openings, τ_c, was the same as the time constant of desensitization, τ_d (see also Colquhoun and Hawkes, 1982). It was shown further that in cell-attached recordings the mean cluster length was in the same range as the τ_d values reported by us and by Dilger and Brett (1990) and Dilger and Liu (1992). Cluster lengths in the 100-ms range also have been reported by Colquhoun and Ogden (1988) for frog muscle at 10–12°C on application of high ACh concentrations. If corrected for the 10°C difference in temperature, then these cluster lengths also conform to the τ_d values found by us. It may be concluded that the short time constants of desensitization observed in outside-out patches reflect a physiological state of the channel. As reported above, desensitization sometimes becomes more rapid by a factor of up to two in the first minutes after excision of a patch. This may indicate that channels in the excised patches are sometimes slightly altered due to excision from the cell membrane.

Desensitization in the quisqualate type, glutamatergic channels of crayfish and locust muscles (Dudel et al., 1990a, b, c), should have a mechanism different from that in the ACh-ergic channels investigated here. In the glutamatergic channels, complete desensitization can occur without channel opening and thus seems to start predominantly from the resting state or from a liganded state close to the resting state. Linear reaction schemes of this type were modeled by Standly et al. (1993). Similar difficulties are encountered as with our scheme 2 in the present article. In the most extensively studied type of crayfish channel (Dudel et al., 1990a), the recovery from desensitization is about as fast as the onset of desensitization, with time constants of a few milliseconds in both directions at high glutamate concentrations. However, the steady-state rate of opening is almost zero, i.e., the affinity of the desensitized channel state for glutamate is much higher than that of the nondesensitized states. In spite of this, $p_{o, max}$ is $\sim$1 for high glutamate concentrations. It seems probably, therefore, that also in case of glutamate, a circular reaction scheme has to be used. This scheme, however, must show essential differences to scheme 3.

REFERENCES

Blan, H., and C. Webster. 1981. Isolation and characterization of human muscle cells. *Proc. Natl. Acad. Sci. USA.* 78:5623–5627.

Cachelin, A. B., and D. Colquhoun. 1989. Desensitization of the acetylcholine receptor of frog end-plates measured in a vaseline-gap voltage clamp. *J. Physiol. (Lond.).* 415:159–188.

Caratsch, C. G., and F. Eusebi. 1990. Effect of Calcitonin gene-related peptide on synaptic transmission at the neuromuscular junction of frog. *Neurosci. Lett.* 111:344–350.

Colquhoun, D., and A. G. Hawkes. 1981. On the stochastic properties of single ion channels. *Proc. R. Soc. Lond. B. Biol. Sci.* 211:205–235.

Colquhoun, D., and A. G. Hawkes. 1982. On the stochastic properties of bursts of single ion channel openings and of clusters of bursts. *Proc. R. Soc. Lond. B. Biol. Sci.* 300:1–59.

Colquhoun, D., and B. Sakmann. 1985. Fast events in single-channel currents activated by acetylcholine and its analogues at the frog muscle end-plate. *J. Physiol. (Lond.).* 369:501–557.

Colquhoun, D., and D. C. Ogden. 1988. Activation of ion channels in the frog end-plate by high concentrations of acetylcholine. *J. Physiol. (Lond.).* 395:131–159.

Dilger, J. P., and R. S. Brett. 1990. Direct measurement of the concentration- and time-dependent open probability of the nicotinic acetylcholine receptor channel. *Biophys. J.* 57:723–731.

Dilger, J. P., and Y. Liu. 1992. Desensitization of acetylcholine receptors in BC3H-1 cells. *Pfluegers Arch. Eur. J. Physiol.* 420:470–485.

Dudel, J., Ch. Franke, and H. Hatt. 1990a. A family of glutamatergic, excitatory channel types at the crayfish neuromuscular junction. *J. Comp. Physiol. A. Sens. Neural Behav. Physiol.* 166:757–768.

Dudel, J., Ch. Franke, and H. Hatt. 1990b. Rapid activation, desensitization and resensitization of synaptic channels of crayfish muscle after glutamate pulses. *Biophys. J.* 57:533–545.

Dudel, J., Ch. Franke, H. Hatt, R. L. Ramsey, and P. N. R. Usherwood. 1990c. Glutamatergic channels in locust muscle show a wide time range of desensitization and resensitization characteristics. *Neurosci. Lett.* 114:207–212.

Fatt, P. 1950. The electromotive action of acetylcholine at the motor end-plate. *J. Physiol. (Lond.).* 111:408–422.

Feltz, A., and A. Trautmann. 1980. Interaction between nerve-related acetylcholine and bath applied agonists at the frog end-plate. *J. Physiol. (Lond.).* 299:533–552.

Feltz, A., and A. Trautmann. 1982. Desensitization at the frog neuromuscular junction: a biphasic process. *J. Physiol. (Lond.).* 322:257–272.

Fiekers, J. F., D. S. Neel, and R. L. Parsons. 1987. Accelaration of desensitization by agonist pre-treatment in the snake. *J. Physiol. (Lond.).* 391:109–124.

Franke, Ch., H. Hatt, and J. Dudel. 1986. The excitatory glutamate activated channel recorded in cell-attached and excised patches from the membranes of tail, leg and stomach muscles of crayfish. *J. Comp. Physiol. A. Sens. Neural. Behav. Physiol.* 159:591–609.

Franke, Ch., H. Hatt, and J. Dudel. 1987. Liquid filament switch for ultra-fast exchanges of solutions at excised patches of synaptic membrane of crayfish muscle. *Neurosci. Lett.* 77:199–204.

Franke, Ch., H. Hatt, and J. Dudel. 1991a. Steep concentration dependence and fast desensitization of nicotinic channel currents elicited by acetylcholine pulses, studied in adult vertebrate muscle. *Pfluegers Arch. Eur. J. Physiol.* 417:509–516.

Franke, Ch., H. Hatt, H. Parnas, and J. Dudel. 1991b. Kinetic constants of the acetylcholine (ACh) receptor reaction deduced from the rise in open probability after steps in ACh concentration. *Biophys. J.* 60:1008–1016.

Franke, Ch., H. Hatt, H. Parnas, and J. Dudel. 1992a. Recovery from rapid desensitization of nicotinic acetylcholine receptors-channels on mouse muscle. *Neurosci. Lett.* 140:169–172.

Franke, Ch., D. Költgen, H. Hatt, and J. Dudel. 1992b. Activation and desensitization of embryonic-like receptor channels in mouse muscle by acetylcholine concentration steps. *J. Physiol. (Lond.).* 451:145–158.

Hamill, O. P., A. Marty, E. Neher, B. Sakmann, and F. J. Sigworth. 1981. Improved patch-clamp techniques for high-resolution current recordings from cells and cell-free membrane patches. *Pfluegers Arch. Eur. J. Physiol.* 391:85–100.

Huganir, R. L., and P. Greengard. 1987. Regulation of receptor function by protein phosphorylation. *Trends Pharmacol. Sci.* 8:472–477.

Jackson, M. B. 1988. Dependence of acetylcholine receptor channel kinetics on agonist concentration in cultured mouse muscle fibres. *J. Physiol. (Lond.).* 397:555–583.

Katz, B., and S. Thesleff. 1957. A study of "desensitization" produced by acetylcholine at the motor end-plate. *J. Physiol. (Lond.).* 138:63–80.

Magazanik, L. G. 1989. Postsynaptic potentiation in neuromuscular junction. *In* Neuromuscular Junction. L. C. Sellin, R. Libelius, and S. Thessleff, editors. Elsevier, Amsterdam, The Netherlands.

Magazanik, L. G., E. E. Nikolsky, and R. A. Giniatullin. 1984. End-plate currents evoked by paired stimuli in frog muscle fibres. *Pfluegers Arch.* 401:185–192.

Miles, K., D. T. Anthony, L. L. Rubin, P. Greengard, and R. L. Huganir. 1987. Regulation of nicotinic acetylcholine receptor phosphorylation in rat myotubes by forskolin and cAMP. *Proc. Natl. Acad. Sci. USA.* 84:6591–6595.

Ochoa, E. L. M., A. Chattopadhgyay, and M. G. McNamee. 1989. Desensitization of the nicotinic acetylcholine receptor: molecular mechanisms and effect of modulators. *Cell. Mol. Neurobiol.* 9:141–178.

Parnas, H., M. Flashner, and M. E. Spira. 1989. Sequential model to describe nicotinic synaptic current. *Biophys. J.* 55:875–884.

Ruzzier, F., and M. Scuka. 1985. The sensitivity of acetylcholine receptors during prolonged neuromuscular activity in the frog. *J. Physiol. (Lond.).* 368:104P.

Ruzzier, F., and M. Scuka. 1986. The effect of repetitive neuromuscular activity on the sensitivity of acetylcholine receptors. *Pfluegers Arch. Eur. J. Physiol.* 406:99–103.

Schuetze, S. M., and L. W. Role. 1987. Developmental regulation of nicotinic acetylcholine receptors. *Annu. Rev. Neurosci.* 10:403–457.

Scuka, M., and J. W. Mozrzymas. 1992. Postsynaptic potentiation and desensitization at the vertebrate end-plate receptors. *Prog. Neurobiol. (NY).* 38:19–33.

Sine, S. M., and J. H. Steinbach. 1984. Agonists block currents through acetylcholine receptor channels. *Biophys. J.* 46:277–284.

Sine, S. M., and J. H. Steinbach. 1986. Activation of acetylcholine receptors on clonal mammalian BC3H-1 cells by low concentrations of agonist. *J. Physiol. (Lond.).* 373:129–162.

Sine, S. M., and J. H. Steinbach. 1987. Activation of acetylcholine receptors on clonal mammalian BC3H-1 cells by high concentrations of agonist. *J. Physiol. (Lond.).* 385:325–360.

Sine, S. M., and P. Taylor. 1982. Local anaestheticas and histrionicotoxin are allosteric inhibitors of the acetylcholine receptor. *J. Biol. Chem.* 257:8106–8114.

Standly, C., R. L. Ramsey, and P. N. R. Usherwood. 1993. Simulation of the gating kinetics of a desensitizing glutamate receptor of locust muscle in response to agonist concentration jumps. *Biophys. J.* In press.

Thesleff, S. 1955. The mode of neuromuscular block caused by acetylcholine, nicotine, decamethonium and succinylcholine. *Acta. Physiol. Scand.* 34:218–231.

Verdoorn, T. A., N. Burnashev, H. Monyer, P. H. Seeburg, and B. Sakmann. 1991. Structural determinants of ion flow through recombinant glutamate receptor channels. *Science (Wash. DC).* 252:1715–1718.